



ANALYSIS OF AIRCRAFT ROLLING OVER POTHoles AND RUTS

Jose E. Gómez Viñas

*Airbus Defence & Space / TEAYY Landing Gear Domain
John Lennon s/n, 28906 Getafe (Madrid) Spain
jose-esteban.gomez-vinas@airbus.com*

Jose M. Chorro Martínez

Airbus Defence & Space / TEAYY Landing Gear and Ground Loads Domain

Angel Martínez Pérez

Airbus Defence & Space / TEAYY Landing Gear and Ground Loads Domain

Silvia Parra Adan

Airbus Defence & Space / TAECD Aeroelasticity and Structural dynamics Domain

Alvaro Ros Contreras

ALTRAN engineering / Landing Gear and Ground Loads Domain

KEYWORDS: Dynamic Loads, Rut, Pothole, Landing Gear, Flight Test, A400M.

NOMENCLATURE:

CBR	California Bearing ratio	A/C	Aircraft
EBH	Equivalent Bump Height	MLG	Main landing Gear
FWD	Forward	NLG	Nose Landing Gear
MID	Middle	MTW	Maximum Take Off Weight
AFT	Rear	MLW	Maximum Landing Weight
SC	Servicing Class		

ABSTRACT

The aircraft A400M has the capability to operate on unpaved runways. As part of the demonstration of this feature, it is necessary to make analysis of the aircraft rolling over runway profiles that could contain potholes and ruts. The A400M aircraft has a non-conventional landing gear in which the main landing gear (LH and RH) consists of three independent articulated-type struts positioned along the aircraft longitudinal axis. As the legs are positioned along the aircraft in the longitudinal axis, during the rolling over potholes and ruts the vertical load distribution between the three legs is changing during the rolling over the potholes and ruts. The complexity of the landing gear is increased as all the struts have a twin wheel arrangement, fitted to the main fitting by a trailing arm assembly.

The analysis of these features is required by two reasons: aircraft safety and operator costs. Aircraft safety is affected because in the case that the ultimate loads of the landing gears are exceeded a collapsing of the landing gears will occur with the consequent loss of the aircraft controllability on ground. In this case a runaway could occur at aircraft high speeds with hazardous or catastrophic consequences. If this operation is only permitted at low speeds without safety impact, damages incurred on the aircraft imply maintenance and repair costs for the operator.

Regulations of civil aircrafts include discrete load conditions (CS25.491 and FAR25.491) that cover the analysis of potholes and ruts. In the case of civil runways exists an inspector that should know the dimensions of the runway and taxiway safety areas at the airport. At airports certificated under Part 139, the dimensions of the safety areas should be documented in the airport certification manual. During the safety area inspection, the inspector should determine if there are any hazardous ruts or a pothole. The airport is responsible for establishing a schedule for regular and routine pavement inspections to ensure all areas are thoroughly inspected.



In the case of military aircrafts operating in unpaved runways, two options could be followed: to define the limitations of the aircraft in terms of pothole and rut size or to comply with the requirements defined in a specific aerodrome regulation. In the first option is needed to define which are the maximum size of the ruts and potholes the airplane can transverse. In the second option, the airplane is designed for crossing the potholes and ruts defined in the aerodrome manual. In both cases, the inspection of the runways has the capability to decide whether the pothole or the rut should be repaired after the measurements of the dimensions.

For the A400M aircraft, it has been followed the first option, i.e. definition of the potholes and rut sizes that the aircraft can cross. This information is included in aircraft characteristics for airport planning manual (ACAP) so the aerodrome director can use it to introduce the runway repairs when needed. It is interesting the methodology followed in the A400M because allows defining in a simple manner the aircraft operation over potholes and ruts. First at all, an aircraft model has been built capable to calculate the landing gear loads during the potholes and ruts crossing. Taking into account the results of the model, it has been generated a list of flight test cases necessary for the model validation. Once the model has been validated with a set of flight test cases, it is possible to define the aircraft limitations for any of the aircraft operating conditions.

The flight tests were performed with different aircraft configuration in order to capture the effects of different aircraft parameters: aircraft weight, centre of gravity position, aircraft longitudinal speed, braking and thrust.

1. INTRODUCTION

This paper summarizes the model description and its validation of A400M military Aircraft into the operation over potholes and ruts in unpaved runways. The more difficulty of this task is the matching of local tyre deformation and also its associated ground deformation near the obstacle area when the wheel is passing over it and which are the parameters that are controlling this phenomenon.

This paper also includes the capability of the aircraft operating with these ground discontinuities based on the previous validation to cover the operations independently of CBR. The capability is taken into account the A/C operation and different variations of the discontinuities like rut shapes and crossing angle.

2. TEST DESCRIPTION

2.1 Requirements

This test was carried out to support a model validation built to cover the capability of the A400M military and tactical aircraft to operate over ground discontinuities like ruts or potholes on unpaved runways.

The ground operations include taxiing at different A/C speeds over the obstacles, and slow turning manoeuvres over three ruts built in parallel at the end of the runway.



Figure 1 Picture of paved & unpaved Woodbridge runways

2.2 Test procedure

2.2.1 Ground preparation

A mapping of the ground mechanical properties was measured by means of the CBR test to get a mean value of the runway strength. This mean value resulted in $CBR \approx 7$ (Ref. 3).

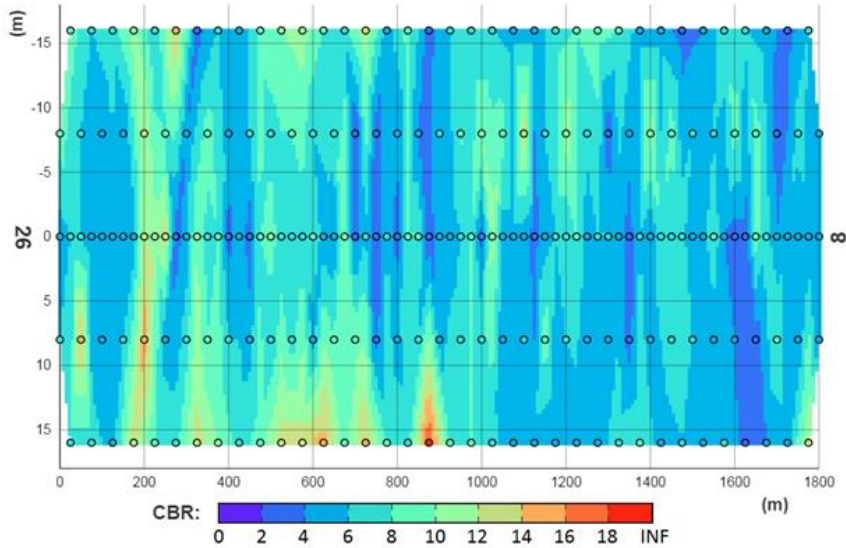


Figure 2 CBR0 map Heat-map – Depth 0 to 10 cm

CAMPAIGN	STATISTICAL PARAMETERS	CBR0	CBR1	CBR2	CBR3	CBR4	CBR5
WOODBIDGE Runway	MIN	2	4	4	2	3	3
	QUARTILE	5	8	7	8	10	9
	AVERAGE	7	11	11	12	14	15

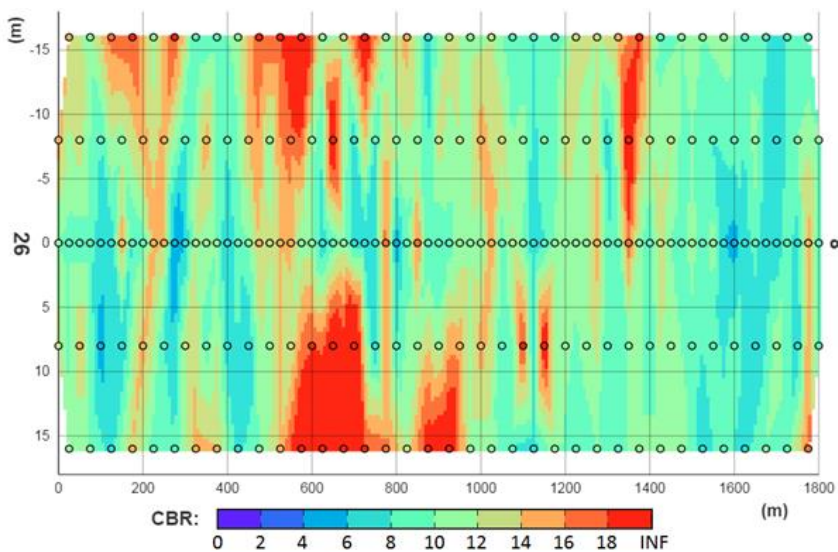


Figure 3 CBR1 map Heat-map. Depth from 10 to 20 cm

Pothole and ruts profiles were defined to be built in the ground as shown in Figure 4 and Figure 5. The following profiles were used as guidance to build the obstacles.

To reproduce the pothole effect and to make easier to the pilot to break through over, a ditch perpendicular to the runway was built. The chosen ditch width of 750 mm is enough to tyre deep into entirely

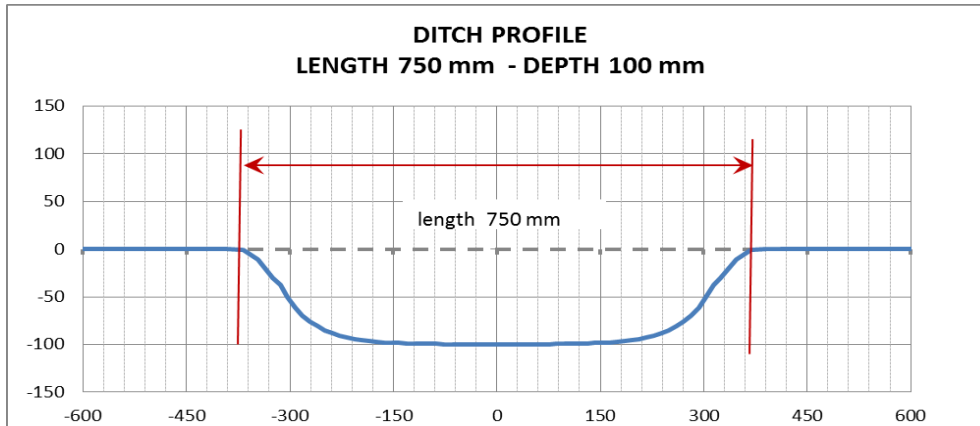


Figure 4: Ditch profile sketch (not to scale)

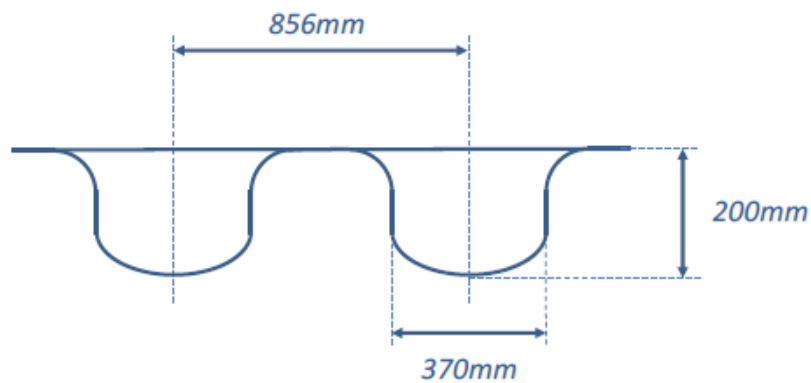


Figure 5: Rut profile sketch (not to scale)

2.2.2 Taxi over pothole and ruts

During the taxi tests, the A/C passed over three different obstacles in the following sequence:

- a) Perpendicular ditch
- b) Rut oriented at 45 deg
- c) Rut oriented at 15 deg

There was a separation of at least 250 m between each obstacle in order to stabilize the shock absorber and to avoid overlapping effect between each dynamic perturbation. (See Ref.2)

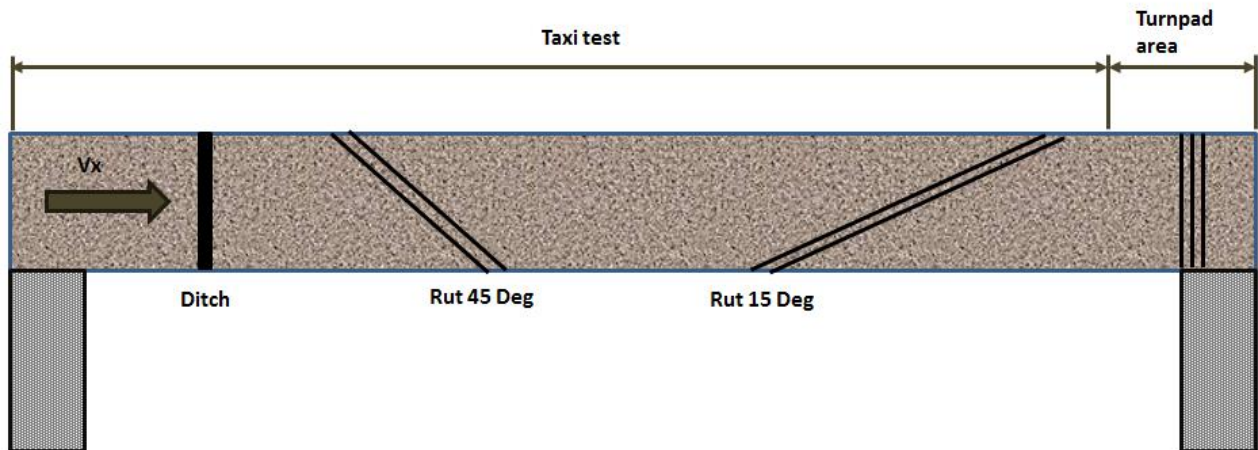


Figure 6: Taxi test layout

As the excitation frequency is important, several A/C speeds were required to evaluate its influence. The test was carried out at four sequential speeds of 10, 20, 40 and 60 knots.

The following table shows the identification of the Taxi tests performed along FT campaign.

TEST	Speed	UTC Initial time	UTC Final time	A/C Weight (Tn)
R0042_1	10Kt	09:56:00	10:02:00	115.2
R0042_1	20Kt	10:28:30	10:32:30	114.2
R0042_1	40Kt	10:48:00	10:50:00	113.6
R0042_2	40Kt	11:39:00	11:43:00	113.1
R0042_3	60Kt	15:06:00	15:08:00	112.2

Table 1 – Taxi tests identification

2.3 Aircraft configuration

The test was performed with A/C A400M MSN002 with complete LG instrumentation

Weight: Between 115 to 112 Tons, Xcg: fwd CG

Tyre pressure servicing class selected below standard servicing pressure for both LGs

This is typical to operate in Low CBR runways.

LG instrumentation is monitorized in the landing gear legs, wheels, structure and A/C attachments.

2.4 Considerations in soft ground

2.4.1 Profile distortion

The tests carried out in Woodbridge (UK) that supports this model were executed in soft ground, with low CBR (Ref.3) which implies high deformations of the ground area near the wheel footprint.

Next picture shows the footprint left behind by the aircraft after passing over the rut during the tests made in Woodbridge.



Figure 7: 15 Deg oriented ruts profile distortion

Here is watched the distortion degree over the terrain made in the original profile when the aircraft is running over it, ending up in a different profile with slopes before and after the hollows. However this picture represents the deformation on the ruts, this consideration is also valid for the pothole profile. Then the mathematical model of the ground profiles has to take into account this degrading of the obstacle original profile by adding the necessary functions over the geometry to can accomplish with. The physical modelling of this dynamic perturbation has been divided in two separated effects.

- Punctual Loads that comes from the corner obstacle
- Loads normal to ground profile along the obstacle.

Deformation characteristics observed along flight tests:

- a) Physical behaviour when the tyre is climbing the obstacle is different to dropping into.
- b) Deformation is higher at lower speeds of the Aircraft
- c) The higher is the deep obstacle, the higher is the terrain deformation.

2.4.2 Loads due to tyre deformation

The vertical force is modelled by the tyre curve function depending on tyre deflection in the general models. This force is perpendicular to ground slope along the whole obstacle and is passing through the wheel centre when the wheel is far from the pothole.

The more difficulty to include in this discontinuity is the fact that vertical force is calculated by a tyre deflection measure in a single point by the normal to surface through the wheel axle, but here in the real life the tyre is going through a very changing profile and a medium deformation is not easy to compute when the terrain changes very quickly.

In order to that, five different deformation phases along the pothole are defined. Drop phase is divided in two alike, bottom phase and the climb phase is also divided into separated ones.

▪ Drop Phase (1)

First phase of the discontinuity occurs where slight slope appears on the ground when wheel is close to the corner of the pothole.

This phase is domain by its length and drop associated. Run length is represented by "Lcorner" and the drop height by "Hcorner" parameters. See **Figure 8**

This slope can represent two different physical effects:

- The geometrical dropping slope of the pothole lateral wall.
- The physical deformation of the soft ground due to tyre vertical load smashing the ground.

This parameter varies according to the longitudinal speed of the aircraft, as mentioned previously in this document. The faster passes the aircraft over the obstacle the lower time to smash the terrain it takes.

For hard runways only the 1st effect is taking into account, while in soft runways both are considered.

- Drop phase (2)

Second stage is drop itself to the bottom level of the pothole. There is a transitory phase between the pothole bottom level and ground level. It represents the transition of the tyre expansion coming from the topside of the pothole into the bottom of it. This effect takes into account that the wheel is not a single point. It has a physical diameter and different differential deformation along the discontinuity so when it is reaching the pothole corner, some of its footprint is still out of the bottom of the pothole when part of it is already in. Therefore a function which joints both height levels is implemented. The length associated to this phase in the model is represented by the parameter called "Lgeo"

- Bottom phase (3)

Third phase represents the bottom level of the pothole where the tyre expands itself and its deflection achieves the minimum value.

- Climb phases (4) & (5)

The climb phase of the wheel is composed for equivalent phases to the drop however the values for the parameters "L_Corner" and "H_Corner" take different values, as the terrain deformation of the profile does not have to be the same.

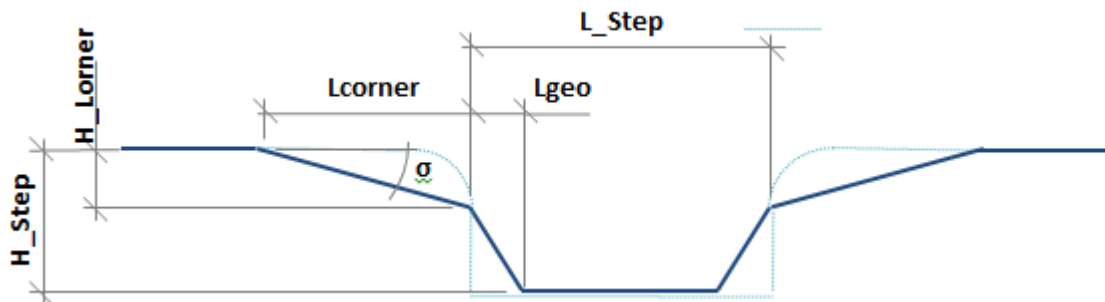


Figure 8: Scheme of the pothole profile

Slope angle:

$$\sigma = \tan^{-1}\left(\frac{H_Lcorner}{Lcorner}\right) \quad (1)$$

For the wheel point of view is much easier drop than climb the obstacle, since the tyre has to clamber for the terrain by mean of terrain deformation as a consequence to struggle the opposition of the gravity and also shock absorber force.

The representation of the wheel centre trajectory when is passing over the pothole, is described below. The expansion of the wheel can be appreciated when reaching the bottom of the pothole.

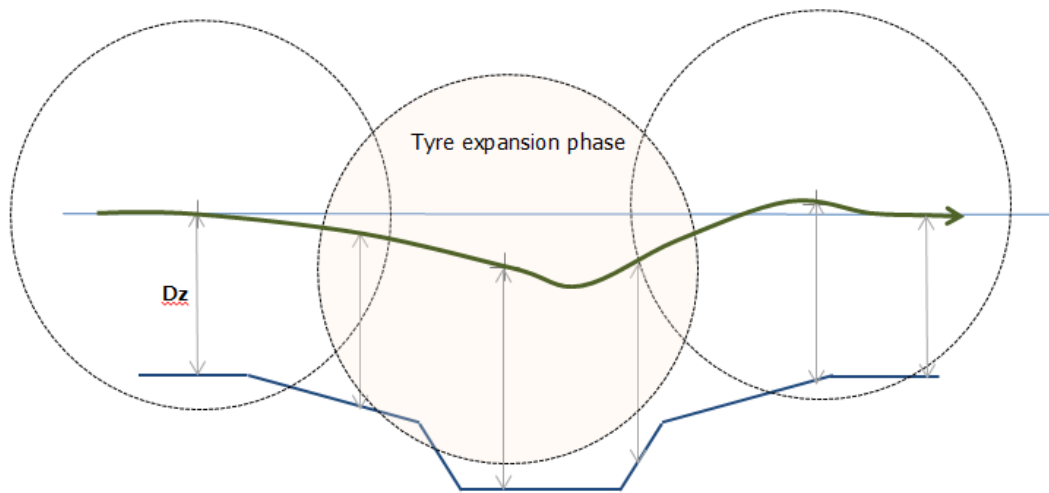


Figure 9: Scheme of wheel centre trajectory

The loads acting along the pothole due to tyre deformations are shown in the following scheme. Three different stages can be found for the vertical load.

- i) During the first stage, before reaching the first slope the Z reaction force is pure vertical.
- ii) When the slope begins, the direction of tyre normal reaction is softly changed with certain angle " σ " equivalent to terrain deformed slope. The deformation length is represented into the model by parameter "Lcorner" and an additional "deltaL" to takes the horizontal component to zero. The process is equivalent during the tyre pothole climbing.
- iii) In the following scheme it is also represented the bottom of the pothole when ground normal force $Fz0$ is applied.

The friction force Ff is assumed as negligible during the flight tests matching process

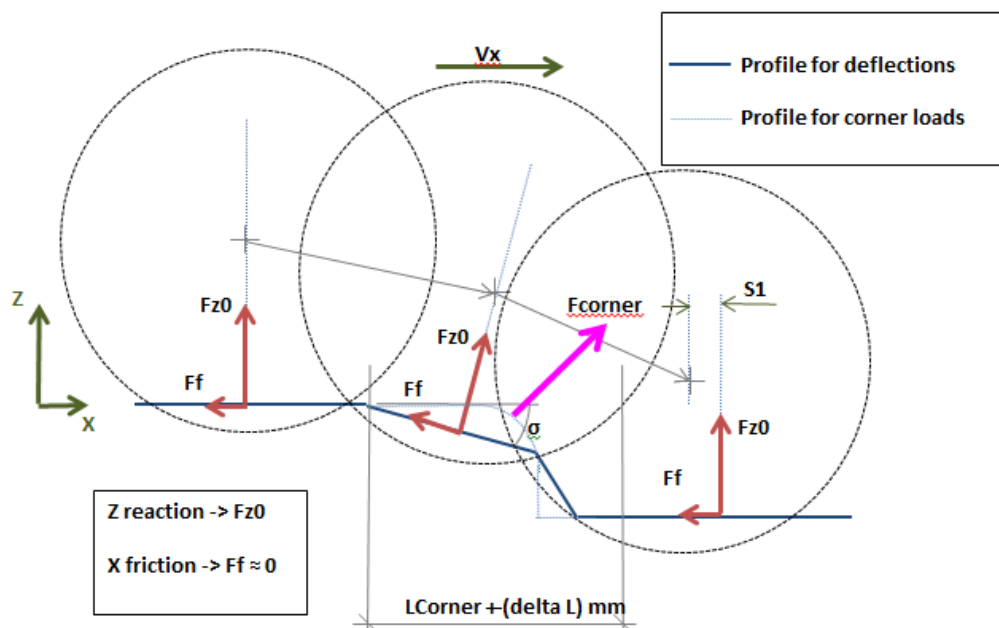


Figure 10: Scheme of loads due to tyre deformation

Formulas of loads due to tyre and ground deformation:

$Fz_0 = f(\text{Pressure, tyre deflection})$ Its projections in ground axes are:

$$Fz_0^z = Fz_0 \cdot \cos(\sigma)$$

$$Fz_0^x = Fz_0 \cdot \sin(\sigma)$$

$F_f = -Fz_0 \cdot \mu \approx 0$ (μ is friction coefficient. No braking forces are applied)

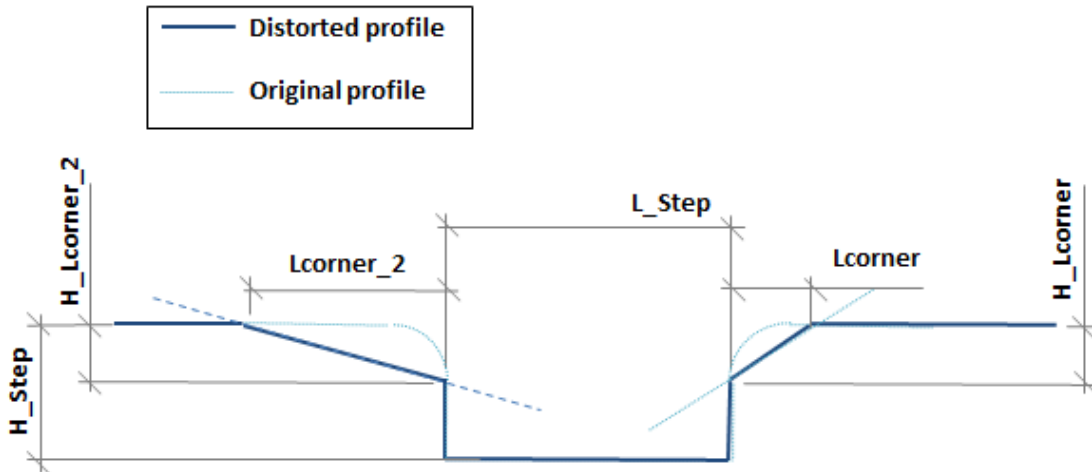


Figure 11: Original profile VS Distorted profile

Parameter suffix with "_2" extension is referring to the drop phase

Deformation follows three rules:

- d) Different physical behaviour when the tyre is climbing the obstacle to dropping into.
- e) The lower is the A/C speed over the obstacle; the higher is the deformation in the terrain.
- f) The deeper is the obstacle, the higher is the terrain deformation.

2.4.2.1 Distortion in the pothole profile depending on A/C speed

As the slope in the pothole climb or drop is defined by two parameters, "Lcorner" & "Hcorner" (Detail view in Figure 12).

After the matching process, the vertical deformation "Hcorner" & "Hcorner_2" was adjusted by keeping constant independently of A/C speed equal to 50 mm.

In the other hand the longitudinal deformation "Lcorner" & "Lcorner_2" is changing with tyre speed as it is described in Figure 13.

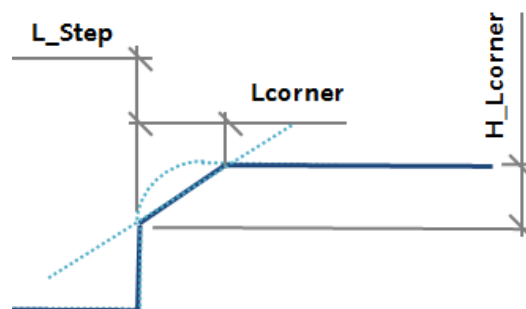


Figure 12: Detail view of climb parameters

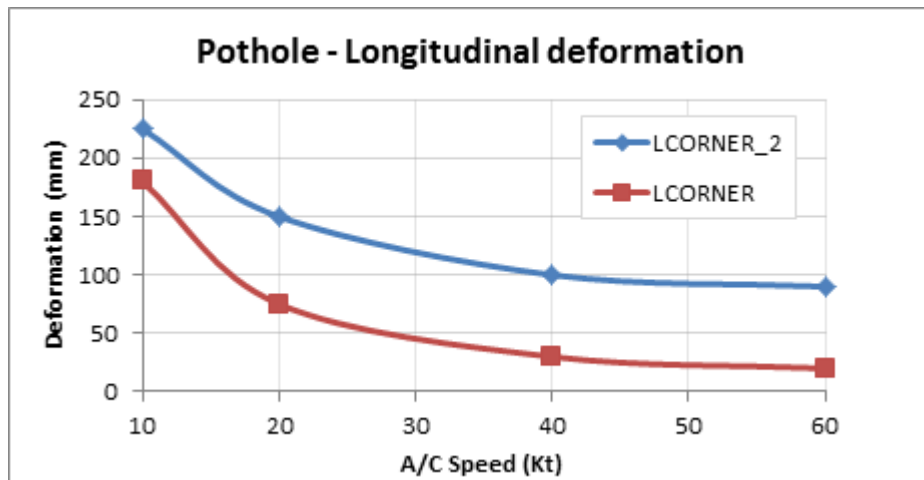


Figure 13: Pothole - Longitudinal deformation

2.4.3 Loads due to corner local deformations

The corner effect over the loads is calculated by the mean deformation on the local area of the tyre surface due to the high profile variations.

- The force reaction FR is not applied pointing at wheel centre point in the model (offset e).
- The force reaction $Fz0$ is not applied pointing at wheel centre point in the model when the wheel approaches the corners (offset $S1$).

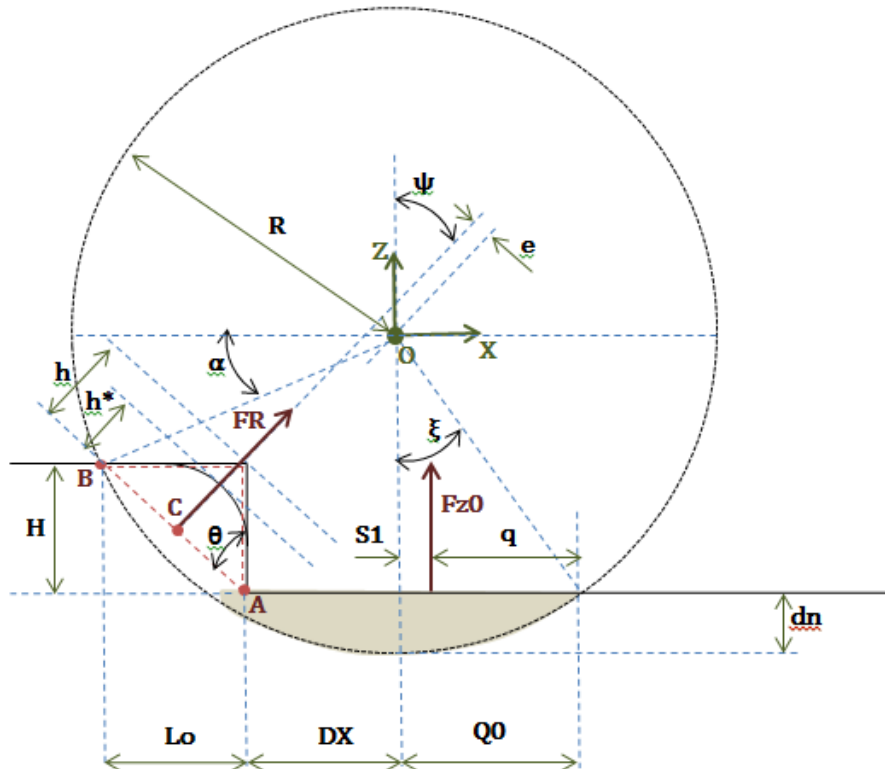


Figure 14: Scheme of mathematical model of vertical force and reaction force in corners

The forces scheme on the tyre shows two separated single forces.

- 1) The first one corresponds to the vertical force "Fz0" on ground. During the impact and along the process when the wheel goes forward through the pothole, the application point of this vertical load is not pointing at the wheel axle. The application point of vertical force is located at middle distance between the step and the end of footprint tyre.
- 2) The second one corresponds to reaction force with the step "FR". It depends mainly of tyre measured deflection "h". In a first approaching, the value of height "h" is taken as the perpendicular distance between the segment "AB" and the perpendicular corner. This value must be corrected by the subtraction of the corner fillet, called "h*".

The next figure represents the detailed area of reaction force modelled in the step. The step profile is shown coloured in red and AB segment length is changing along the time, since "Lo" length is decreasing by the wheel forward advance.

Note: This scheme is only a graphic representation of the mathematical parameter in the pothole corner shaped by triangle (A,B,C)

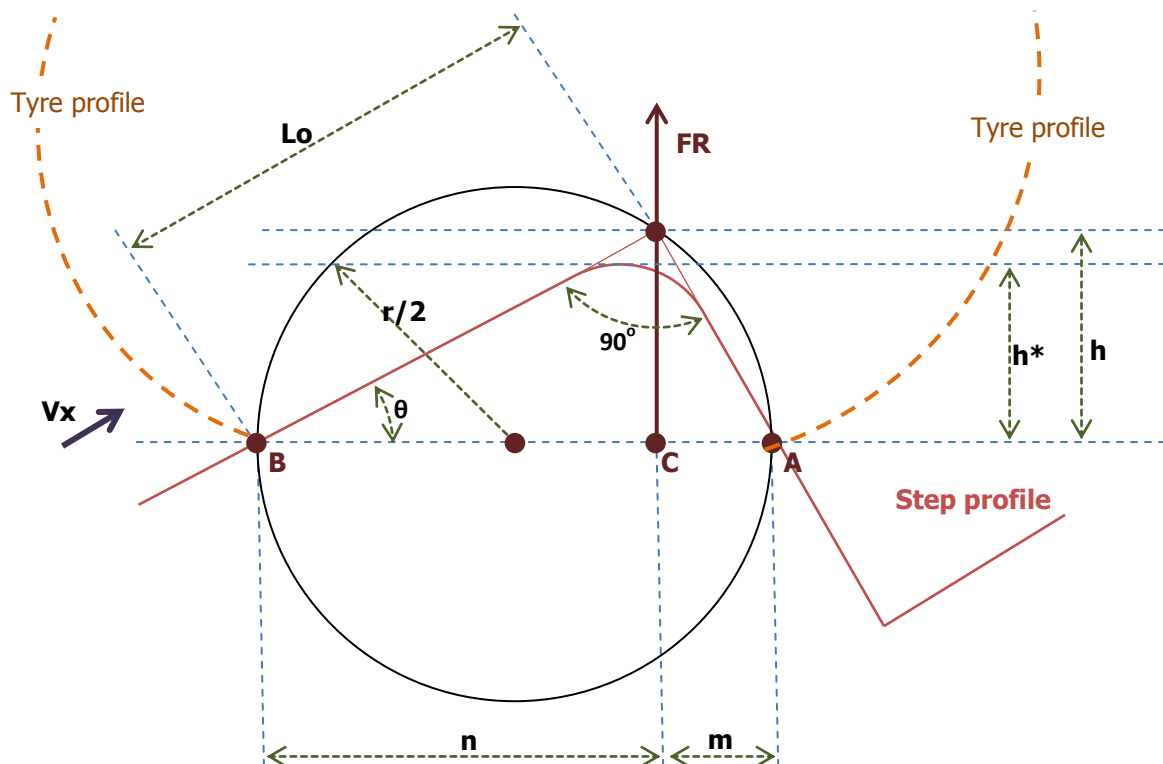


Figure 15: Detailed scheme of mathematical model focused in of corner reaction force

The fillet correction generates a reduction of the reaction force compared with those by a sharp corner. An ellipse mathematical model is used by the implementation of this effect

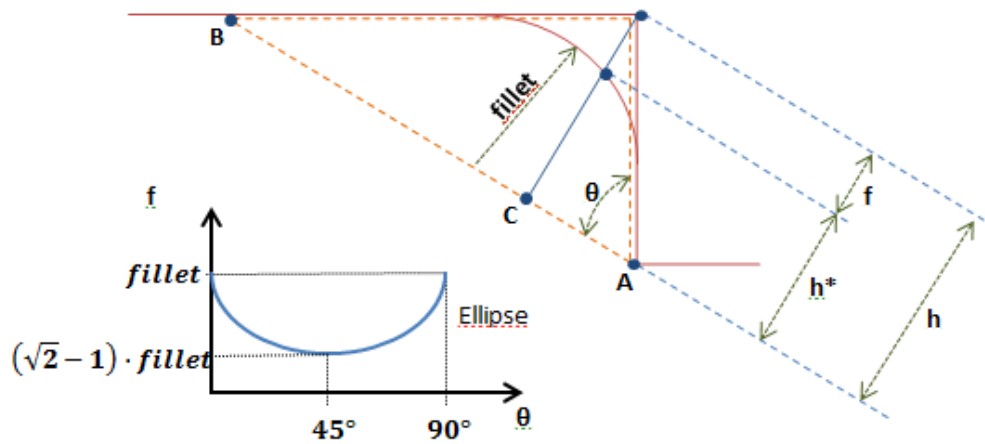


Figure 16: Detailed scheme of mathematical model for h^* parameter

Below are shown the formulas involved in this modification.

h = tire deflection by sharp step
 h^* = corrected tire deflection
 f = fillet subtraction
 fillet = fillet radius

$$h^* = h - f$$

$$f(\theta) \begin{cases} f(0^\circ) = \text{fillet} \\ f(45^\circ) = (\sqrt{2} - 1) \cdot \text{fillet} \\ f(90^\circ) = \text{fillet} \end{cases} \quad (2)$$

In conclusion, the loads applied due to the corners are given by the next expression:

$$FR = K_r \cdot f(\text{Tyre Pressure}, h^*)$$

Where K_r is the coefficient used to adjust the model which represents the CBR effect, in other words, the ground mechanical characteristics.

This flight tests performed were adjusted to $K_r=0.5$ after matching process was ended.

2.4.4 Ground damping

Contrary to paved runways where a rigid non-deformable soil is considered, into the unpaved runway and depending of terrain strength and its plasticity, mechanical characteristics between them are given, like damping effect. This effect is implemented in the model by including a damping between ground and tyre extracting from tested tables into the working study carried out by "The Texas Highway Department" in cooperation with "USA Federal Transportation department".

According to (Ref4), The soil damping factor is expected to vary in function of the soil properties such as humidity, soil composition e.g. in this document it can be found that in unpaved soils the damping coefficient can raise up to $1 \cdot 10^5 \text{ N} \cdot [\text{m}/\text{sec}]$.

To establish a typical value for Woodbridge runway and extracting from Ref.4 table according to Sandy-clay runways a conservative value of 0.6 for damping "J" parameter is selected. This value of damping parameter "J" whose units are expressed in $[\text{ft}/\text{sec}]^{-1}$ is equivalent to $8000 \text{ N} / [\text{m}/\text{sec}]$ with $4 \cdot 10^3 \text{ N}$ of tyre vertical load.

Table XVI
RESULTS OF TESTS ON HALL PIT SANDY-CLAY

Type of Test—unconsolidated undrained
 Confining Pressure—none
 $P_{\text{static}} = 55.3$ pounds
 Moisture Content = 34.68%

$N(\text{optimum}) = 0.11$
 Average J = 0.775

Height of Drop	Velocity of Deformation	Dynamic Load	$\frac{P_d}{P_s}$	J for N = optimum	J for N = 0.18
Inches	ft/sec	pounds			
0.0	1.45	103.0	1.86	0.83	0.81
0.0	1.10	98.4	1.78	0.77	0.77
1.0	3.29	105.8	1.91	0.79	0.74
2.0	4.84	105.8	1.91	0.76	0.69
2.0	4.25	106.9	1.93	0.78	0.72
3.0	6.27	107.0	1.93	0.75	0.67
3.0	6.20	107.0	1.93	0.75	0.67
3.0	6.375	109.1	1.98	0.78	0.70
9.0	10.73	112.2	2.03	0.77	0.67
9.0	11.65	112.8	2.04	0.77	0.67
12.0	11.68	113.0	2.04	0.78	0.67
12.0	11.65	112.8	2.04	0.77	0.67
12.0	11.30	113.0	2.04	0.78	0.67

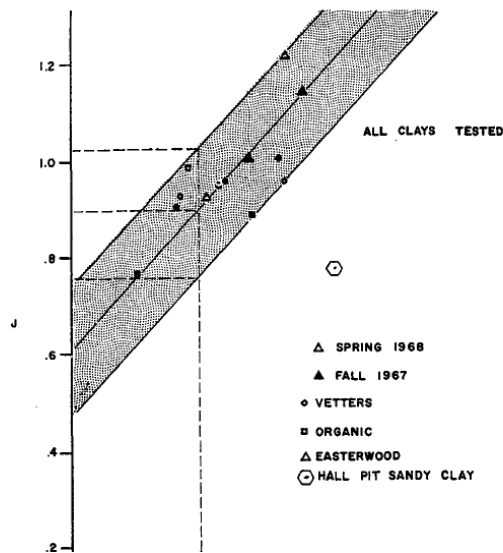


Figure 17: Results of damping tests on hall pit sandy-clay soils

2.5 Modifications to implement Ruts Model

2.5.1 Geometry modifications for Rut model

The double rut profile is basically a double pothole profile separated the geometric distance between twin wheels, with pothole width according to tyre width. This duplication must be incorporated itself the properly changes in its dimensions.

Next scheme shows ruts profile used in the simulations for low CBR runways according to Ref.2 and flight test performed in Woodbridge.

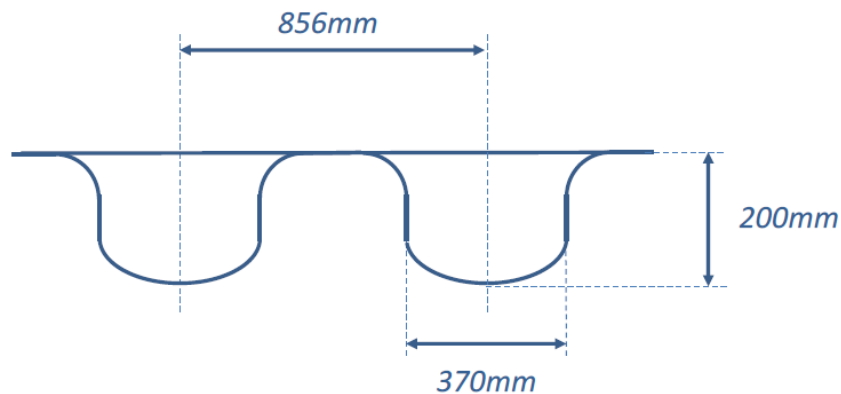


Figure 18: Ruts Profile

2.5.2 Forces modifications for Ruts model

In this way, the ruts have been modelled by duplicating the loads model appearing in the pothole model.

But basically, the main difference between the forces that comes from a taxi over a pothole against the taxi over the ruts is the lateral load component "FY" perpendicular to LG leg that appears if the rut is not perpendicular to the tyre plane.

Other important difference respect to the pothole model comes from the applied sequence of loads. When passing over a rut obstacle with a certain angle, the loads applied on the wheel are not simultaneous at both wheels. This fact produces excitation is higher frequency ranges. In general four different loading state phases can appear:

- Phase A. The right tyre drops into the first rut while its twin wheel stills outside.
- Phase B. Left tyre drops into the first rut while the right one is already in the lateral wandering
- Phase C. Right tyre drops into the second rut while the left one stills in the lateral wandering.
- Phase D. Left tyre drops into the second rut while its twin tyre is already outside.
-

In the following figure it is shown the different phases from A to D respectively: red, purple, blue and light dashed blue.

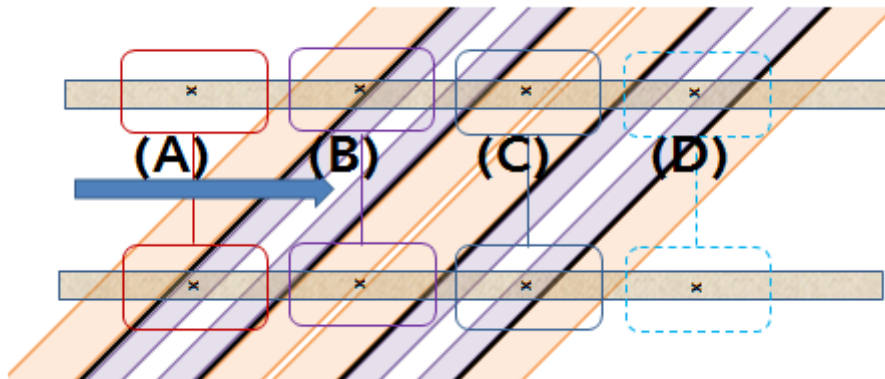


Figure 19: Load phases in ruts obstacle

2.5.3 Implementing the angle between aircraft trajectory and ruts direction

On the contrary to the pothole direction, which is perpendicular to the aircraft trajectory, since it represents physically a hole circular on the ground, in the ruts depending on the trajectory which is facing the tyre against the rut, appears a lateral component of reaction force, and it will be higher, how much more parallel will be the rut with respect to the tyre trajectory. This change introduces modification in the rut length dimension that is seeing the tyre, now it shall be taken as this length the projection on its trajectory.

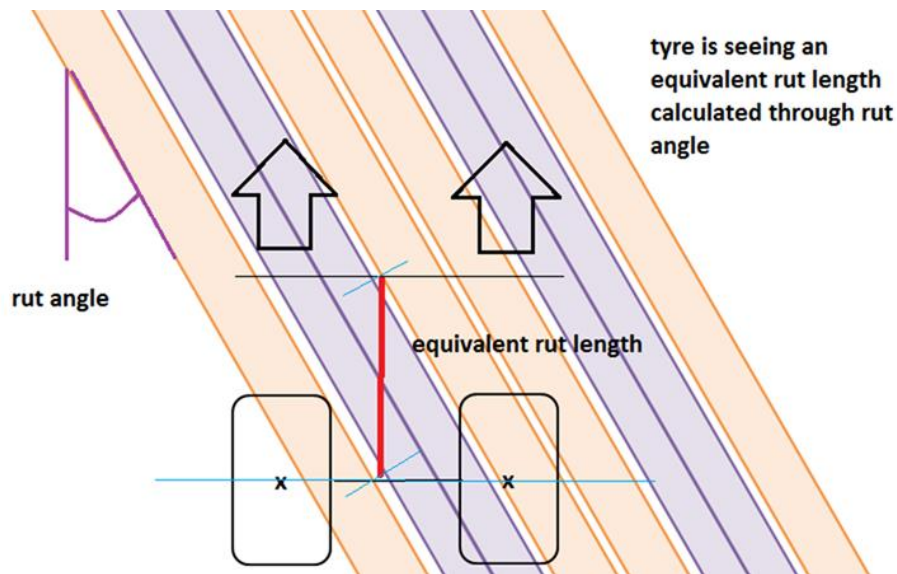


Figure 20: Scheme of equivalent rut length

2.5.4 Tyre Geometry considerations

The parameter "Lgeo" controls the tyre geometric expansion into the pothole or rut. Its adjustment depends on the free space that the tyre finds to can expand itself when it crosses onto the obstacle.

Next picture shows the tyre expansion physical effect taking into account the orientation of rut.

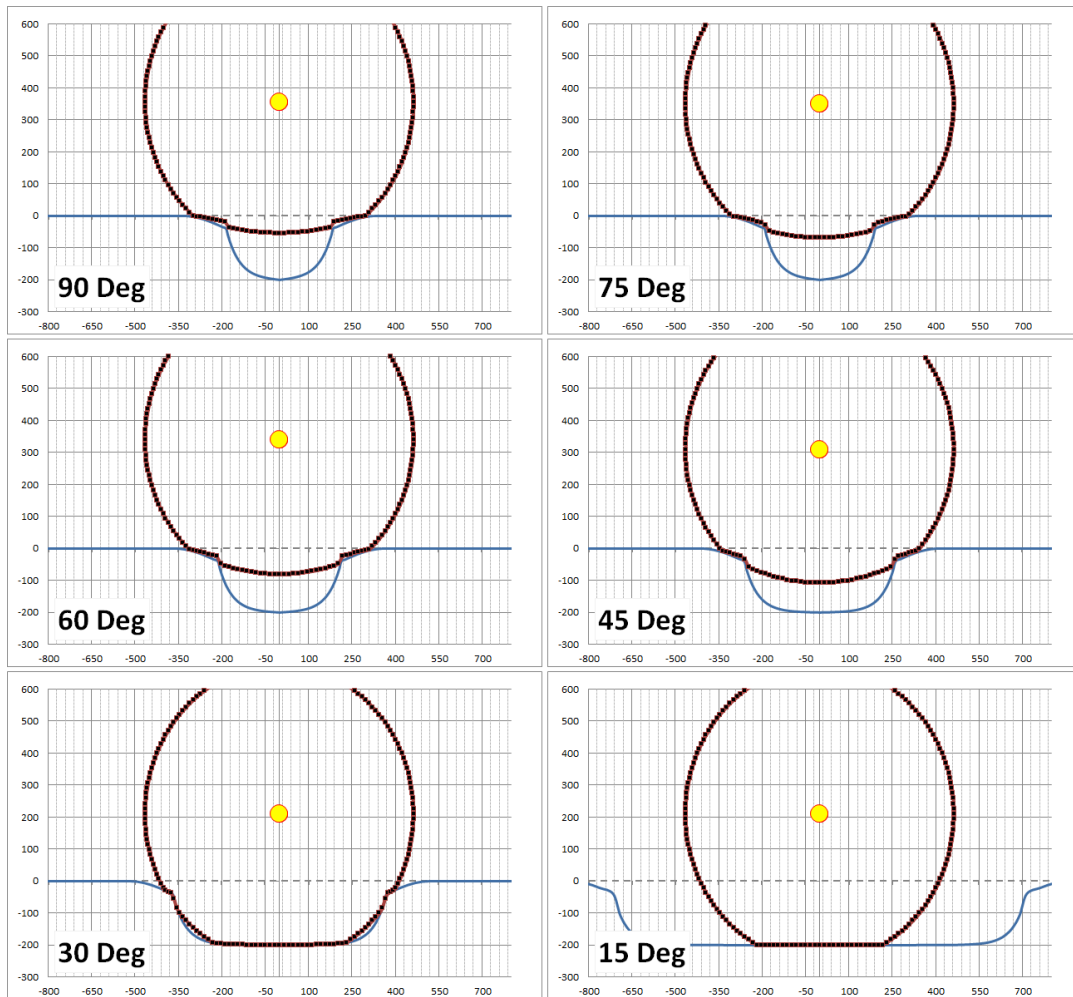


Figure 21: tyre geometric study Vs rut orientation

It is represented a longitudinal section of how the tyre is expanding when it pass over a rut of 370mm.

The tyre does not reach the rut bottom for orientations higher than 30 deg. In these cases the wheel gets at the front corner of the rut before leaving the first one, being supported by the two corners instead of the bottom.

In conclusion, the geometry implications related to the rut orientation effect over its equivalent size-leads to the classification of the ruts angle in three different sectors:

- a) 1st sector which covers the range between perpendicular rut to 60° degrees rut with respect to tyre speed vector.
The tyre passes across over the obstacle without dropping into the bottom of it.
- b) 2nd sector which covers the range between 60° degrees to 30° degrees rut with respect to tyre speed vector
The tyre passes across over the obstacle partially dropping into the bottom of it.
- c) 3rd sector which covers the range between 30° degrees to parallel ruts with respect to tyre speed vector
The tyre passes across over the obstacle by entirely dropping into the bottom of it. The limit case is when the tyre is rolling into the rut which is parallel to tyre speed vector.

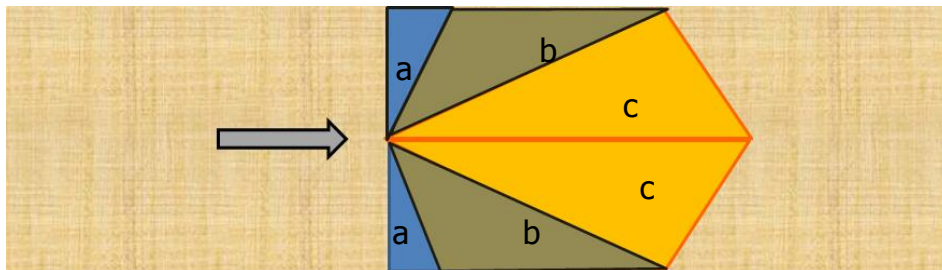


Figure 22: Classification of angle rut sectors along Runway

2.5.5 Effective horizontal ground loads

Regarding to the effective force direction, some other modifications had been implemented respecting the pothole model. In the ruts case, when the rut is not perpendicular to the A/C movement direction, the horizontal load "F_{xy}" is not perpendicular to the rut due to ground deformation is higher in the movement direction. Therefore an effective angle is included as parameter to control the longitudinal load reaction.

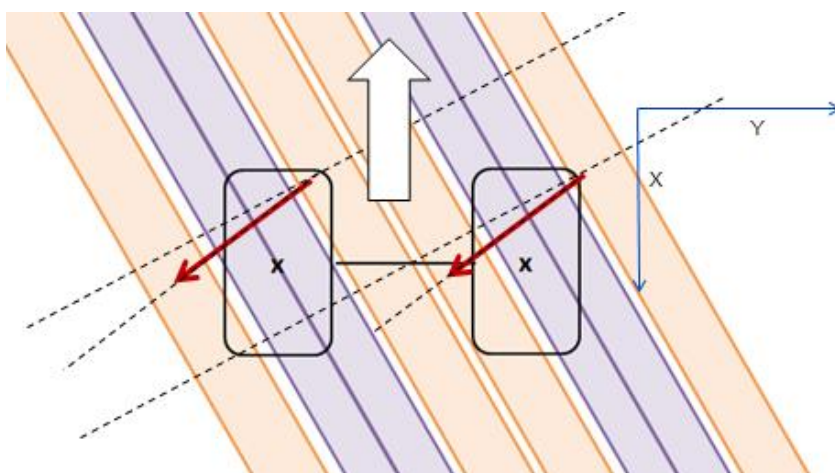


Figure 23: Ruts effective angle

This change in the effective angle depends on the speed of the aircraft, being more pronounced for higher speeds. The physical idea is that the faster impacts the tyre against the rut, the more component over movement direction takes the reaction force.

It also depends on the Rut Angle sector case, having two sectors classified by the fact the tyre enters or not into the rut:

Rut angle ≤ 30 deg \rightarrow The tyre enters completely or partially into the rut

Rut angle > 30 deg \rightarrow the tyre does not enter into the rut

See previous chapter where this is explained with more detail.

This effective angle is implemented by means of a coefficient defined as following:

$$\text{Effective Angle} = \text{Eff}_{\text{angle}} \text{ coefficient} * \text{Rut Angle}$$

This coefficient reduces the real angle in function of A/C speed according to the next table.

Rut Angle $> 30^\circ$	Effective angle coefficient	
	10 kt	0.85
	20 kt	0.67
	40 kt	0.33
	60 kt	0.2

Rut Angle $\leq 30^\circ$	Effective angle coefficient	
	10 kt	0.7
	20 kt	0.6
	40 kt	0.5
	60 kt	0.4

Table 2 - Effective angle coefficient

2.5.6 Slope on climb and drop considerations in relation to speed and rut angle

The slope in the rut due to the ground deformation is defined by two parameters, "Lcorner" & "Hcorner" with different values for drop and climb phase.

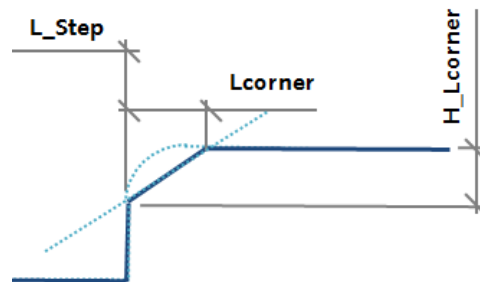


Figure 24: Sketch representing "HCorner" and "LCorner" parameters

The parameter "LCorner" is also changing with respect to the pothole profile. In addition to the three assumptions of ground deformations mentioned in point §2.4.1, in the rut case appears a fourth one taking into account the sector in which the rut angle is found (See §2.5.4).

In concrete, the terrain deformation also varies with the rut angle classification. The variation of these parameters along rut angle is adjusted as follow:

- 1st sector "A" (rut perpendicular to 60 deg) Tyre passes over rut
The parameters value remains constant according to Table (Ω1)
- 2nd sector "B" (rut sector between 60 deg to 30 deg) Tyre partially enters into rut
The parameters value remains constant according to Table (Ω1) from 60 deg to 45 deg
The parameters value varies linearly from 45deg according to Table (Ω1) till 30 deg value of Table (Ω2)
- 3rd sector "C" (rut sector between 30 deg to 0 deg) Tyre completely enters into rut

The parameters value remains constant according to Table ($\Omega 3$) adjusted with test performed at 15 deg

Interpolation guide by rut angle & sectors

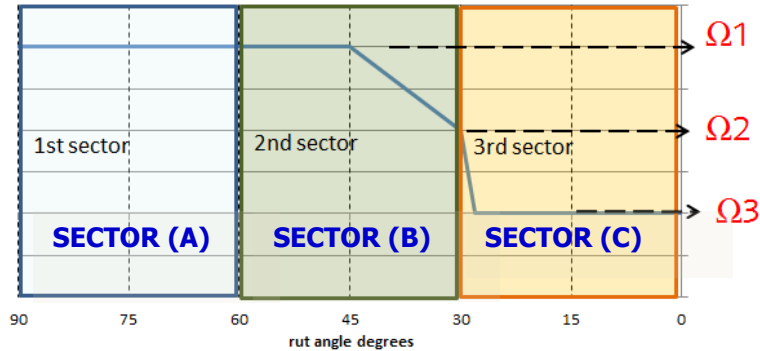


Figure 25: Interpolation procedure by rut angle of "corner" parameters

Extracting the graphs from the tables, it is easier to check that the change in the angle only affects the climb of the pothole.

$\Omega 1$	Speed (Kt)		
	10	20	40
Lcorner_2	225	150	100
Hcorner_2	50	50	50
Lcorner	180	75	30
Hcorner	50	50	50

$\Omega 2$	Speed (Kt)		
	10	20	40
Lcorner_2	225	150	100
Hcorner_2	50	50	50
Lcorner	180	75	30
Hcorner	100	100	100

$\Omega 3$	Speed (Kt)		
	10	20	40
Lcorner_2	225	150	100
Hcorner_2	50	50	50
Lcorner	160	150	50
Hcorner	190	120	110

Table 3 - Corner deformations in rut profile (mm)

Note: The suffix "_2" refers to the drop and non-suffix to the climb of the wheel along the pothole.

This friction force is assumed as negligible during the matching process

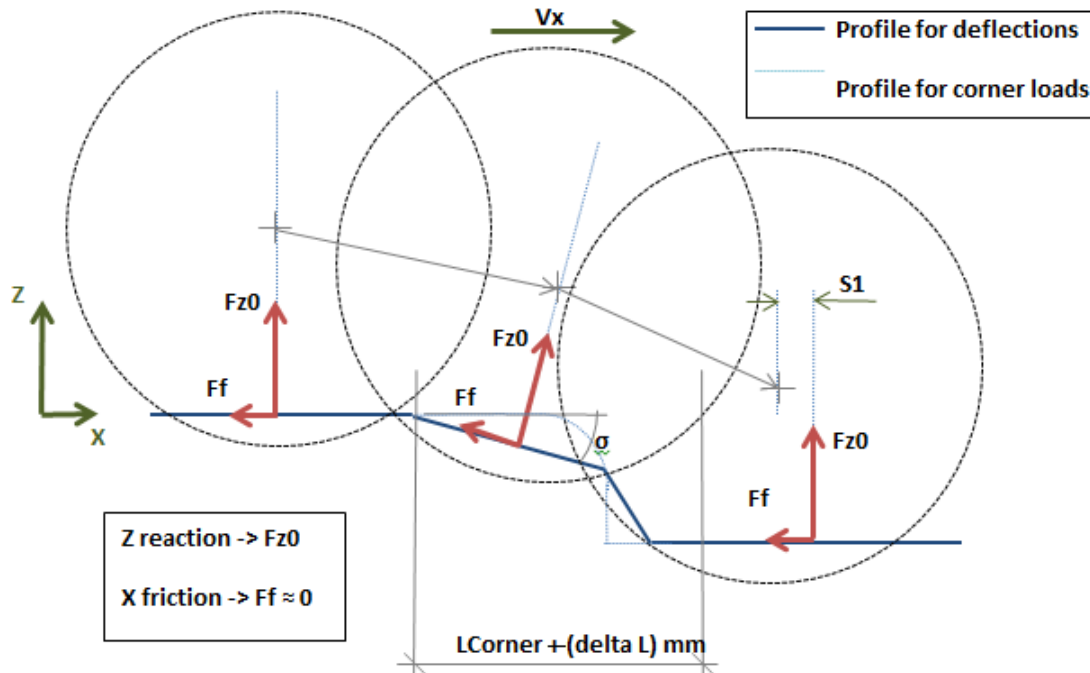


Figure 26: Scheme of loads due to tyre deformation

Formulas of loads due to tyre and ground deformation:

$Fz0 = f(\text{Pressure, tyre deflection})$ its projection expressed in ground: axes are
 $Fz0^z = Fz0 \cdot \cos(\sigma)$
 $Fz0^x = Fz0 \cdot \sin(\sigma)$
 $Ff = -Fz0 \cdot \mu \approx 0$ (μ is the friction coefficient. No braking forces are applied)

3. MODEL VALIDATION

3.1 Pothole profile

Considerations:

- The test was carried out in a soft ground according to measurements reported in Ref.3. It implies that the wheels deform the ground and distort the pothole profile when running over it.
- Neither the CBR is homogeneous along the runway nor the pothole profile is perfectly shaped all along its transversal section, so this could bring discrepancies between the loads obtained and the loads expected.
- When the MLG is running over a pothole, the forward leg distort the pothole profile by generating ruts over its steps, so the middle and after legs do not go through the clean original profile.

The real runway profile (EBH) has not been loaded in the model since the runway has been prepared previously to the performing tests. This mathematical model is focused mainly into the local loads effect in the leg when the tyres break through the obstacle.

The correlation has been checked through following parameters

- The ground loads on the legs measured at wheels axle centre (Fx & Fz)
- Longitudinal links loads on MLG
- Panel links loads on MLG
- Side links loads on MLG
- Total load shared between all NLG dragstay attachments
- Total vertical load measured in NLG main fitting attachments

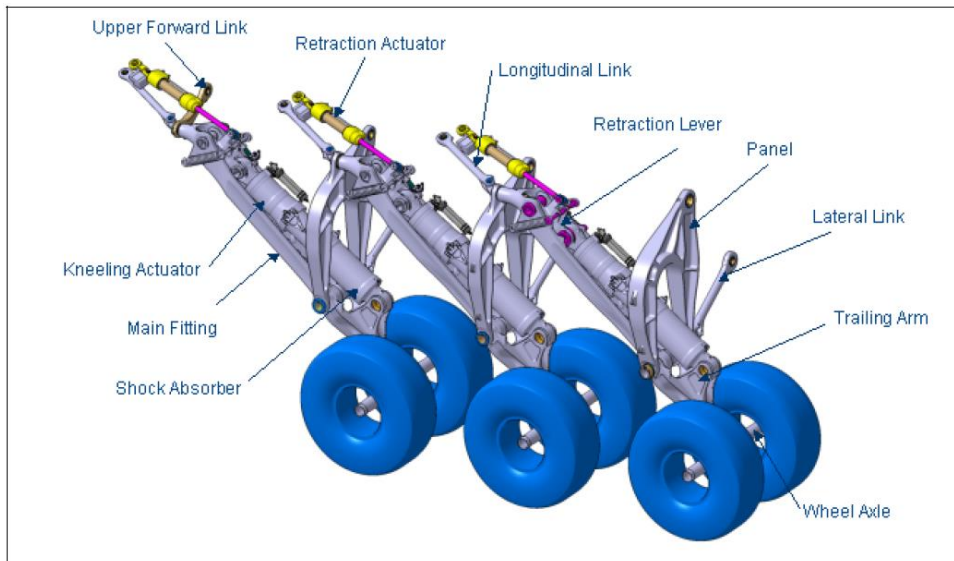


Figure 27: Scheme of MLG structural parts

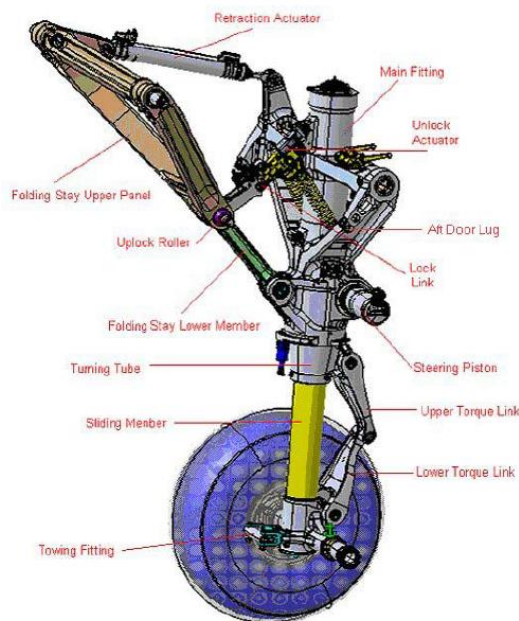


Figure 28: Scheme of NLG structural parts

Next figures are showing the evaluation of matching process in ground loads and attachments

Note: For the validation process, and in order to evaluate isolated the dynamic perturbation of ground obstacles, the static levels have been matched before the excitation.

3.1.1 Case (1) Taxiing over pothole bump at 10kt. Ground Fz & Fx Loads

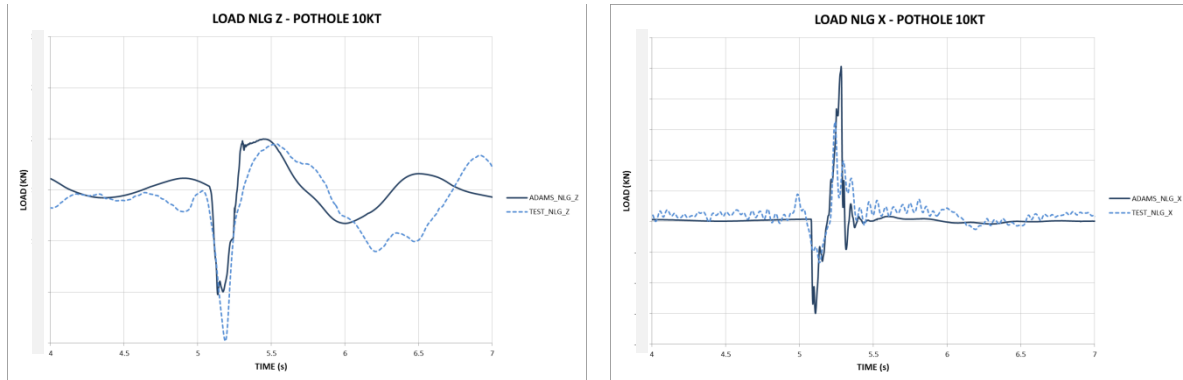


Figure 29: FZ & FX on NLG leg

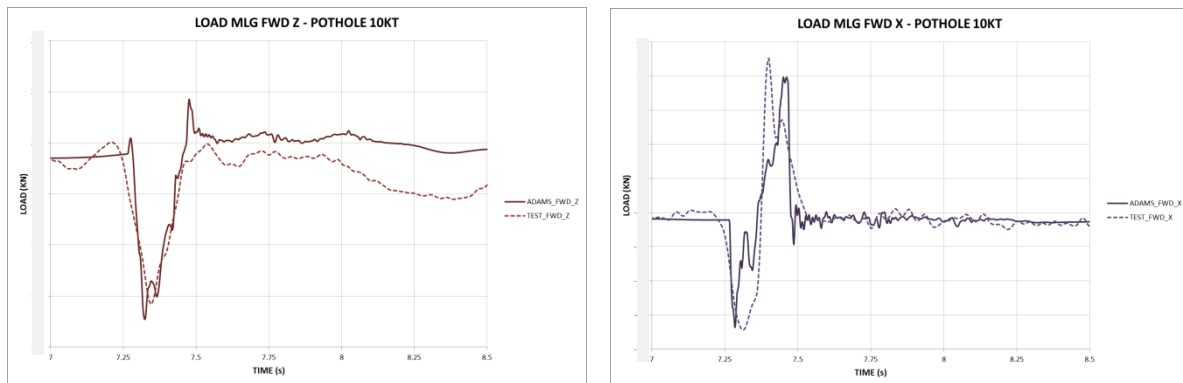


Figure 30: FZ & FX on FWD leg (mlg)

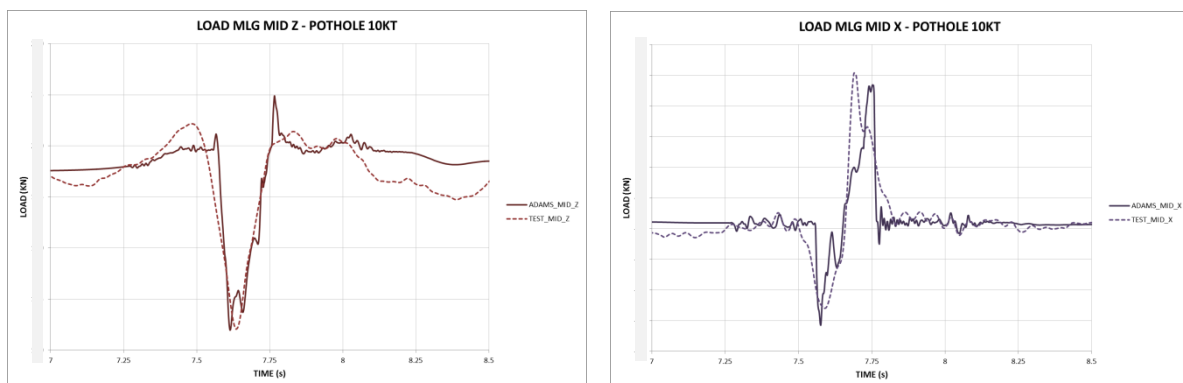


Figure 31: FZ & FX on MID leg (mlg)

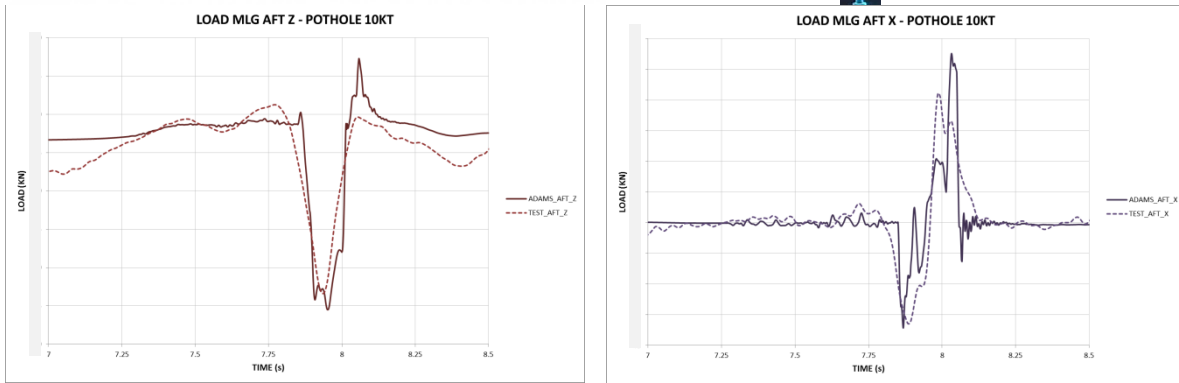


Figure 32: FZ & FX on AFT leg (mlg)

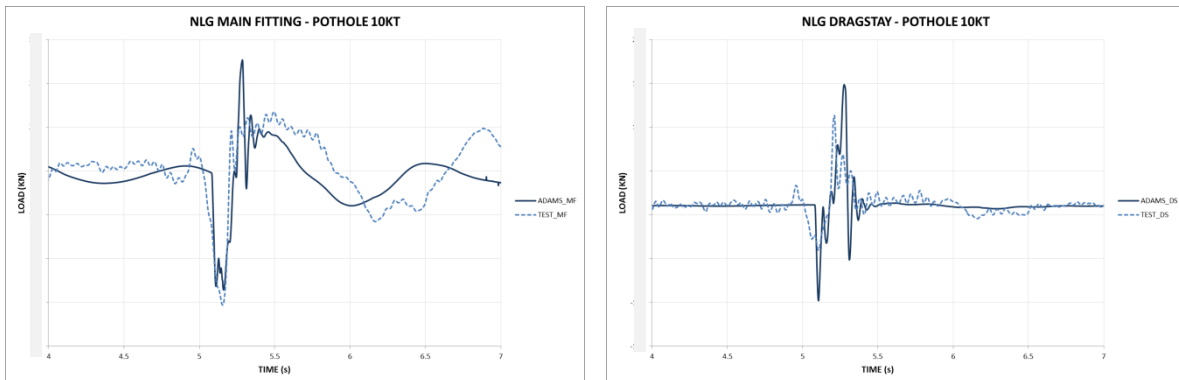


Figure 33: Vertical load at NLG main fitting & bar dragstay load

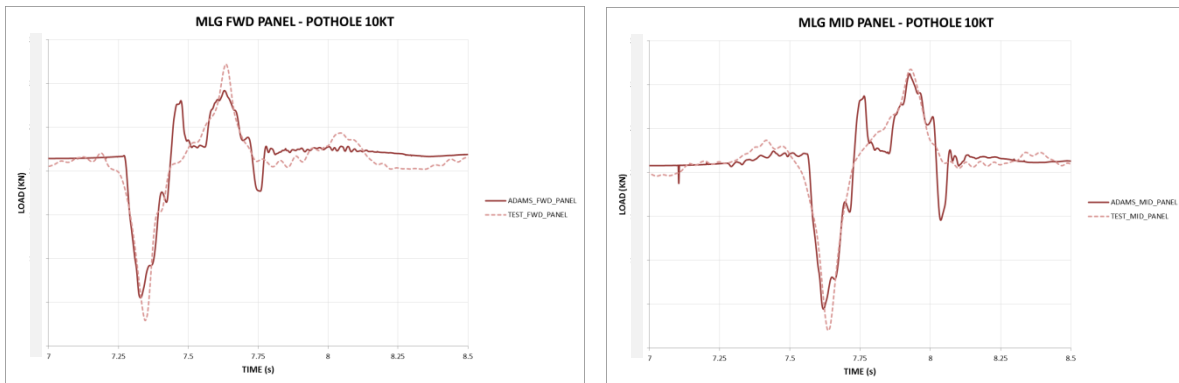


Figure 34: Vertical load on FWD & MID panel

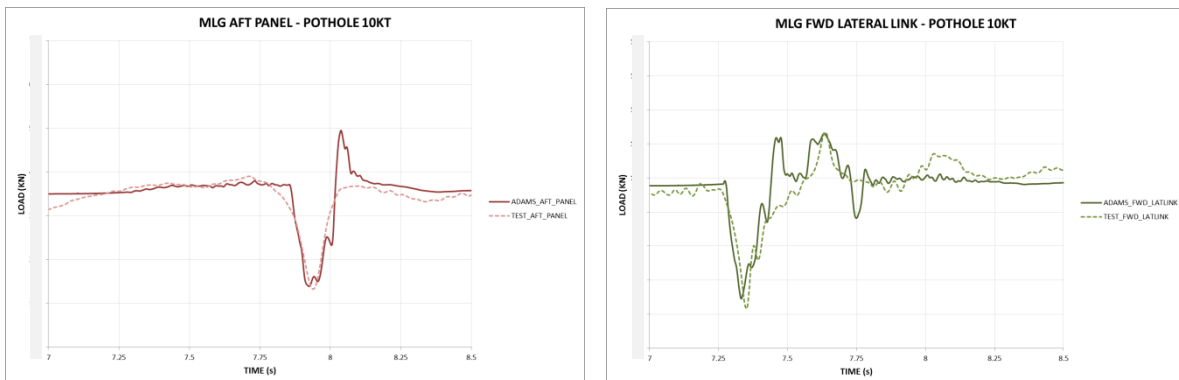


Figure 35: Fz on AFT panel link & FWD lateral link load.

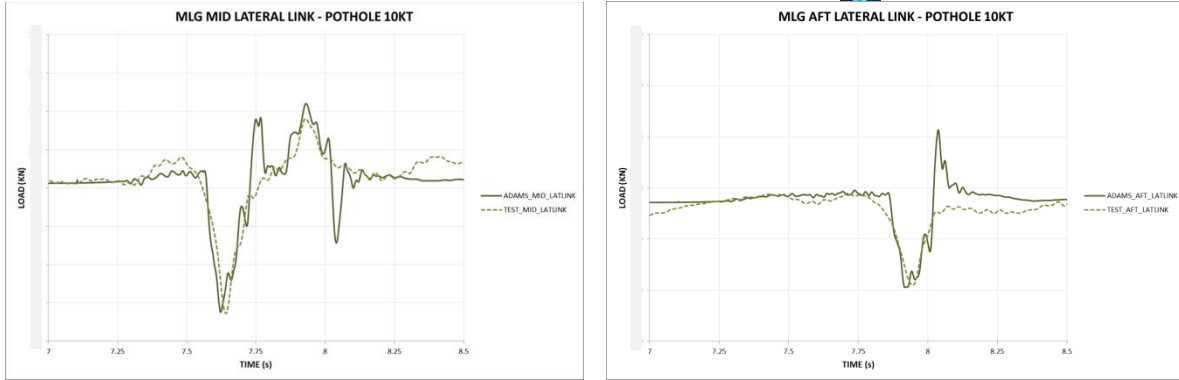


Figure 36: Side load on MID & AFT lateral link.

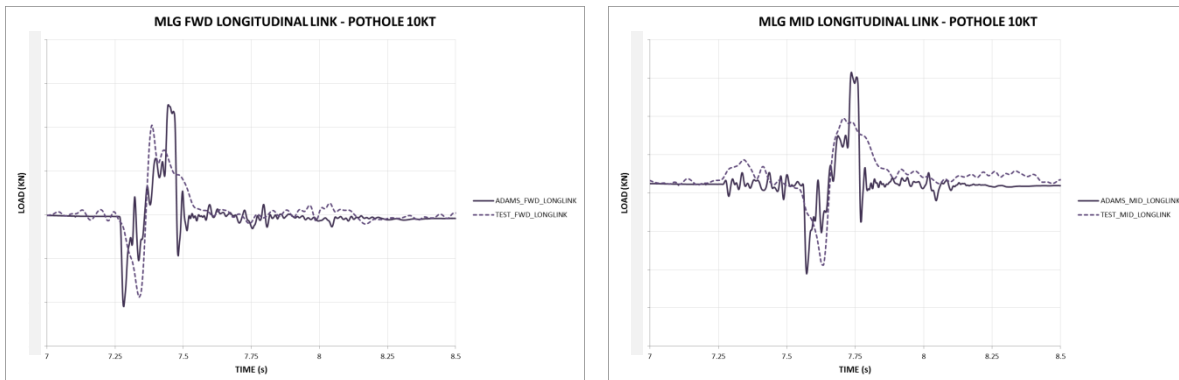


Figure 37: Drag load on FWD & MID longitudinal link.

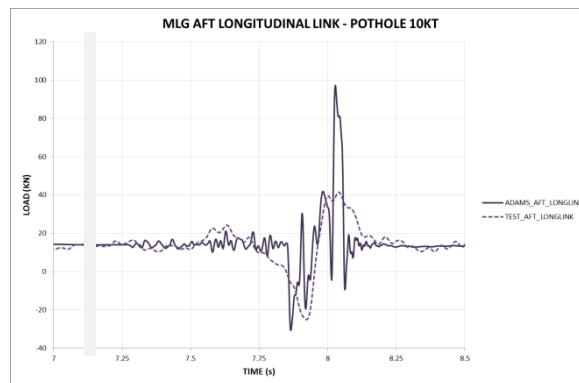


Figure 38: Drag load on AFT longitudinal link.

3.1.2 Conclusion for correlation values of Pothole profile

Due to the huge quantity of time-histories analysed during this matching process, the global evaluation shows enough accuracy level to fulfil the objective.

The dynamic response in peak levels and frequency fulfils a good correlation with flight test results on both landing gears. The matching model is satisfactory as much as qualitative level and quantitative analysis.

The model shows good correlation for the attachment loads either on the NLG and MLG.

Notes:

Only horizontal and vertical loads are considered, since side loads are negligible in this type of obstacles perpendicular to the aircraft longitudinal axis.

3.2 Ruts profile

3.2.1 Rut considerations relevant for the matching process

Main assumptions to take into account for the ruts model

- The test was carried out in the same test campaign as potholes into a soft runway according to Ref.3 It implies that the wheels are passing over the obstacle are going to distort it the outside corners and mainly to destroy partially the lateral wandering.
- Due to stretch space equivalent to width tyre for only one rut when the tyre is passing over it, the tyre is not capable to expand physically into the rut entirely therefore, the parameter that is commanding this effect needs different a properly values for ruts that was used to adjust the pothole. Besides the rut angle when tyre is facing against this itself, affecting the rut length that tyre is watching, and therefore the capability to expand into the rut itself.
- Another relevant effect is the different way that the tyre is climbing the rut, scratching the sand from the rut lateral wall, with respect to dropping phase, much softer for the terrain.
- Neither is the CBR homogeneous along the runway nor is the rut profile perfectly shaped all along its transversal section, so this could bring some discrepancies between the loads obtained and the loads expected.
- When the MLG is running over a rut, the forward leg distort the rut profile by generating ruts over its steps, so the middle and after legs do not go through the clean original profile.
- As it was reported in chapter §2.5.4 the angle effect over the rut size when the tyre is facing for can be classified in three sectors and the limit case is when the tyre is rolling into the rut which is parallel to tyre speed vector.

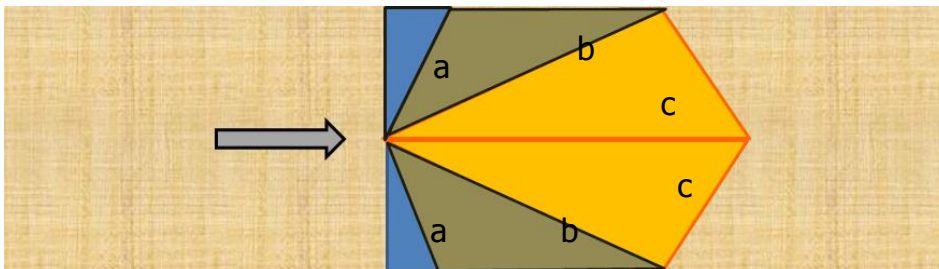


Figure 39: Classification of angle rut sectors along Runway

Performed flight took placed at 45 deg and 15 deg respectively. Therefore the 1st one corresponds to case inside the sector (b) of Figure 39 that means physically partially dropping and the rut, and the other one, rut at 15 deg is classified into the sector (c) with a totally dropping in the rut which corresponds justly with more demanded cases in term of loads.

This separation on angle rut in three sectors helps to apply limitation latterly to run crossing ruts over determinate sectors when the scenario of CBR will be harder than the tested conditions.

- As the same way as pothole model, the real runway profile (EBH) has not been loaded in the model

The correlation has been checked through following parameters

- The ground loads on the legs measured at wheels axle centre (Fx, Fy & Fz)
- Longitudinal links loads on MLG
- Panel links loads on MLG
- Side links loads on MLG
- Total load shared between all NLG dragstay attachments
- Total vertical load measured in NLG main fitting attachments

Note: For the validation process, and in order to evaluate isolated the dynamic perturbation of ground obstacles, the static levels have been matched before the excitation.

3.2.2 Case (6) Taxiing over Ruts 15 Deg at 40kt

All the plots including the ADAMS tool angle which the is complementary of $15^\circ \rightarrow 75^\circ$

3.2.2.1 Ground Fz, Fx & Fy Loads on wheel axle centre (Ruts crossing 15° , 40kt)

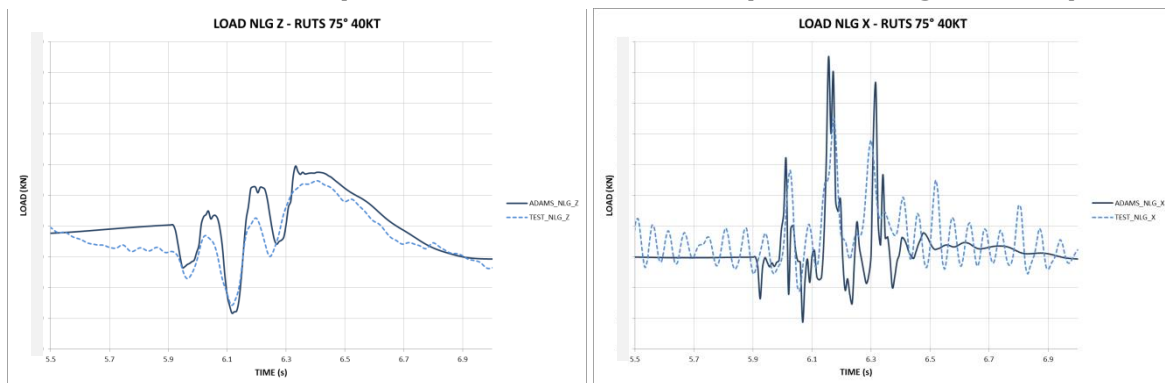


Figure 40: FX & FZ on NLG leg

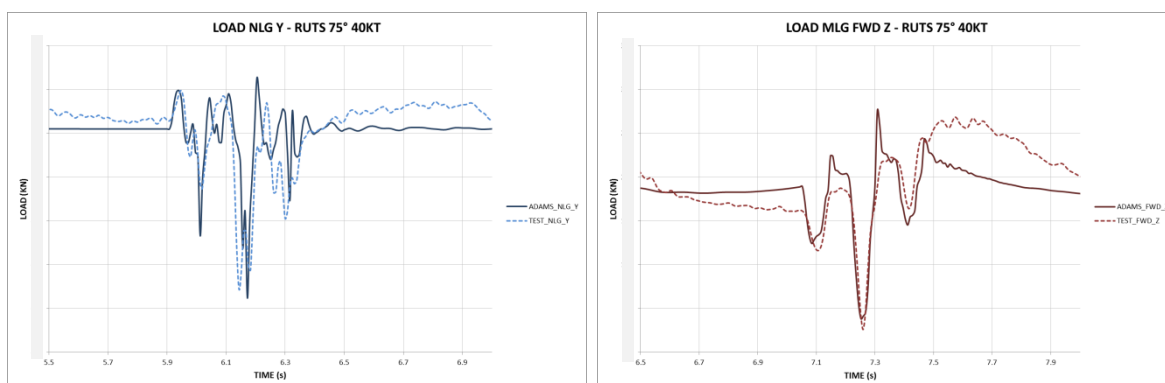


Figure 41: Side load of NLG leg

Vertical load on FWD leg (mlg)

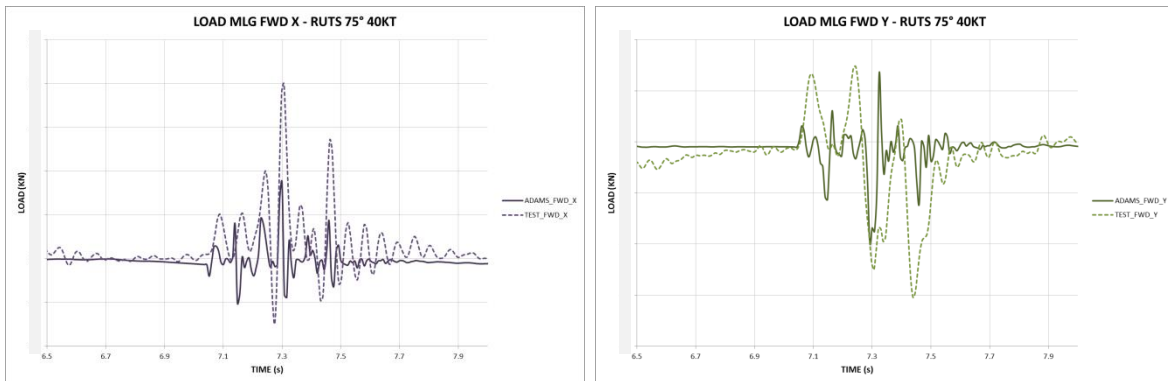


Figure 42: Drag load and side load of FWD leg (mlg)

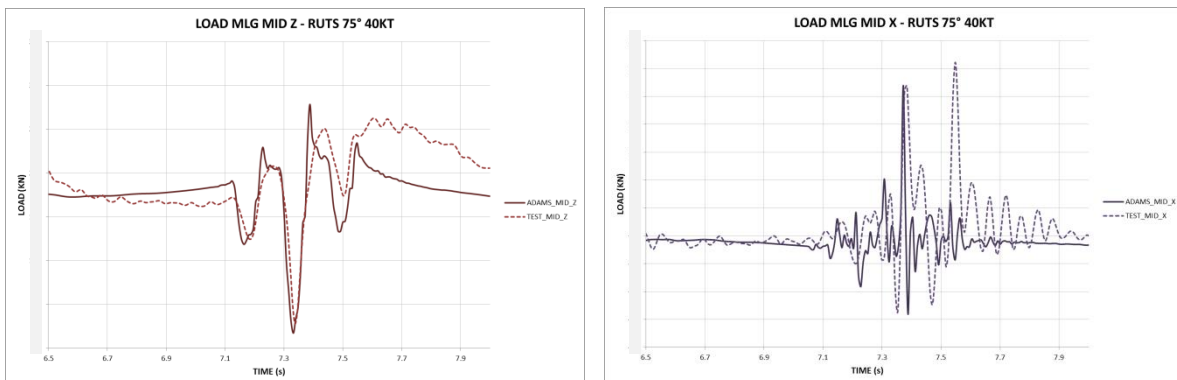


Figure 43: FX & FZ on mid leg of MLG

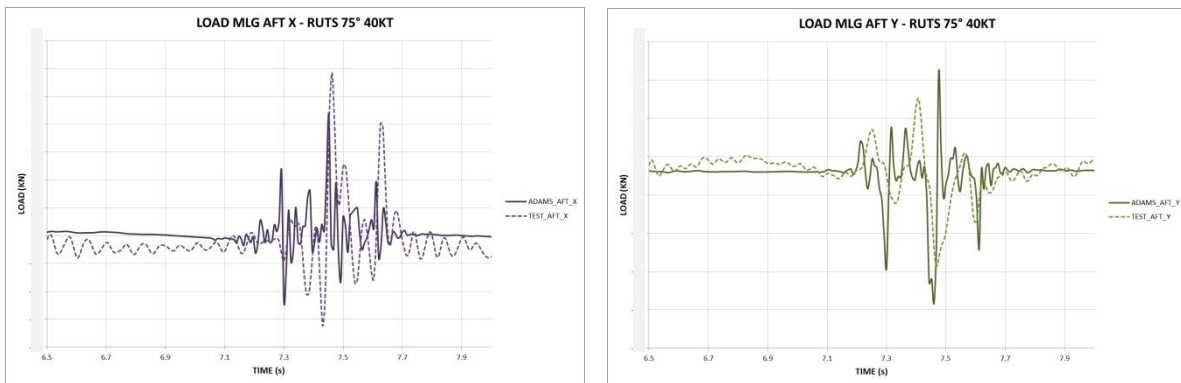


Figure 44: Drag load and side load of AFT leg (mlg)

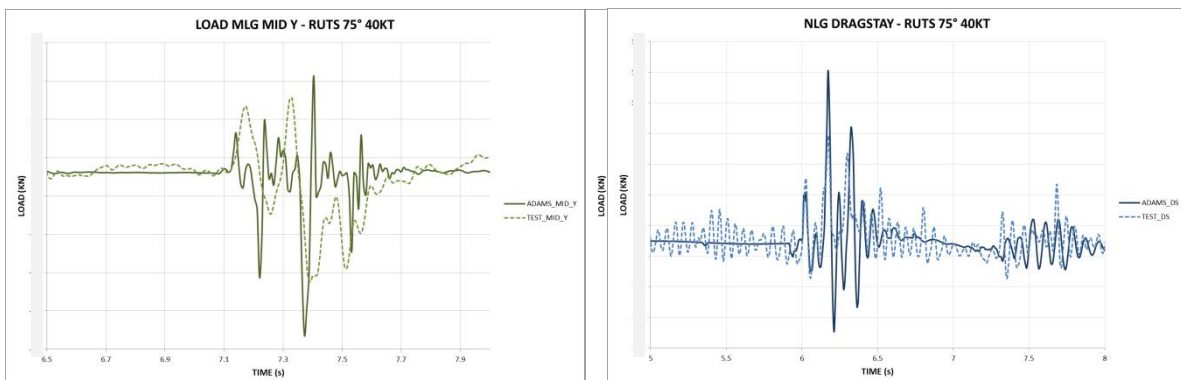


Figure 45 FZ reaction NLG main fitting and dragstay pintles

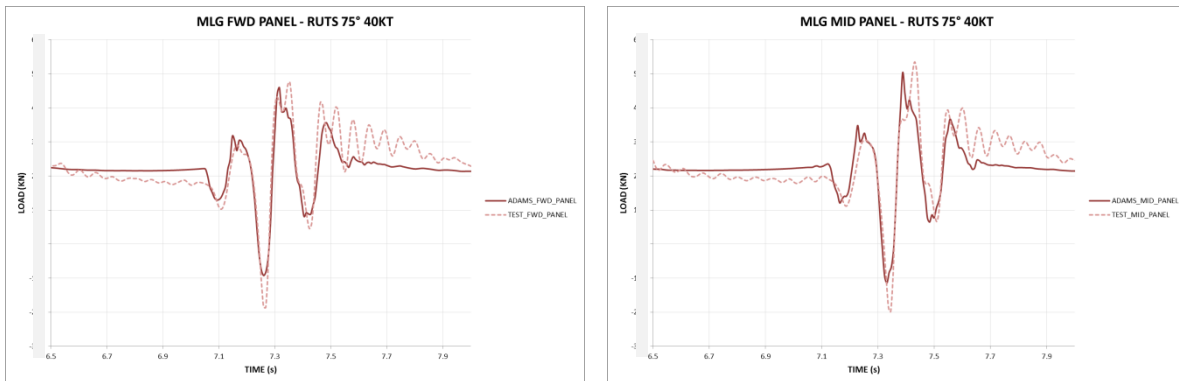


Figure 46: Vertical load on FWD & MID panel link.

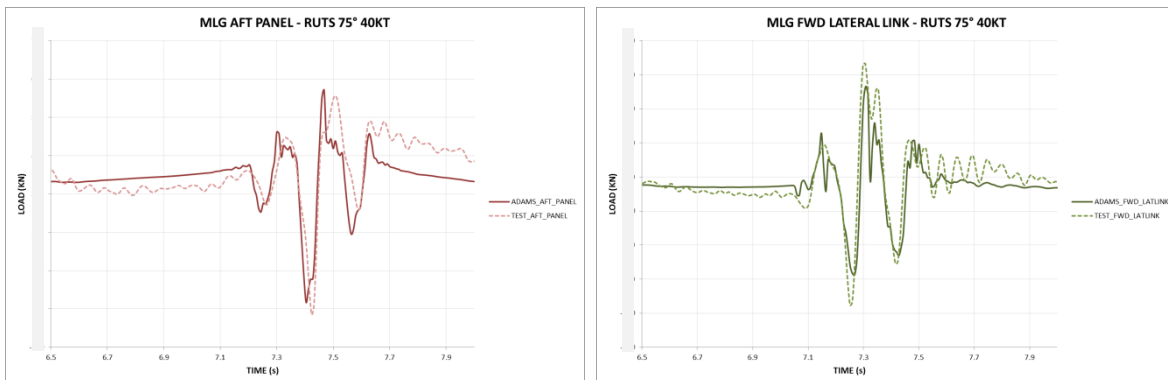


Figure 47: Vertical load on AFT panel and FWD lat. link

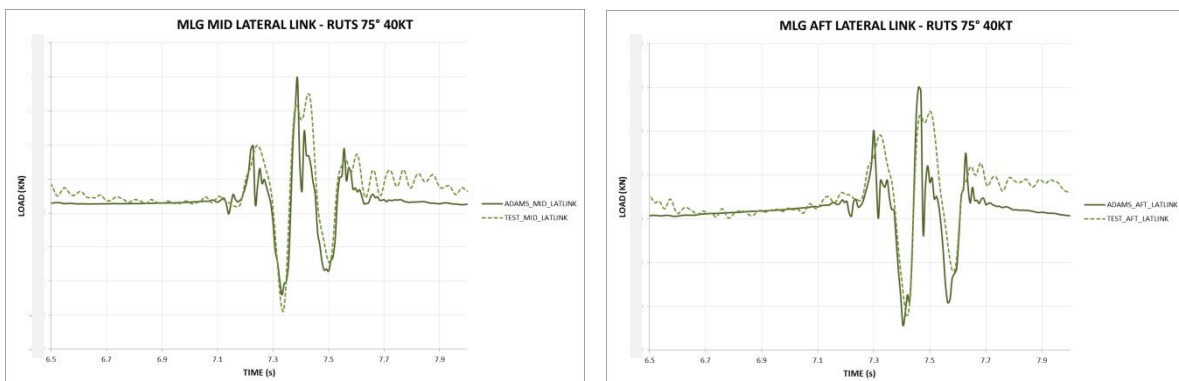


Figure 48: Side load on MID & AFT lateral link

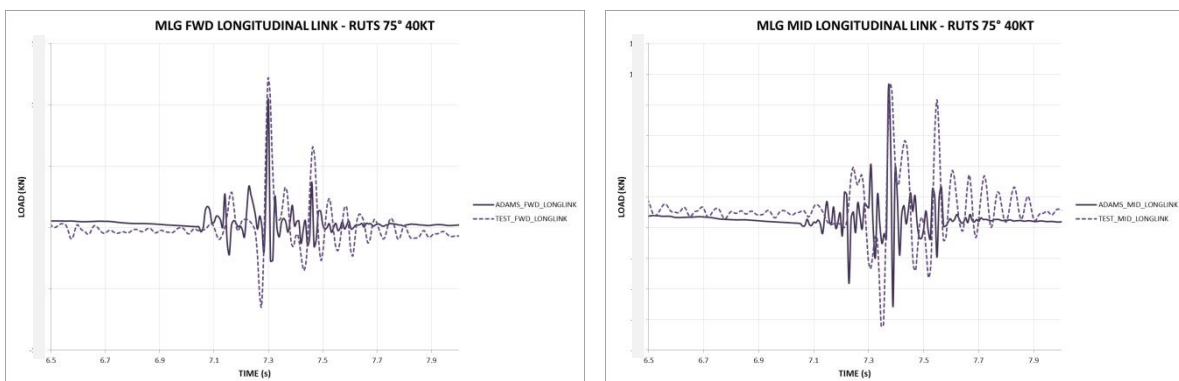


Figure 49: Drag load on FWD & MID longitudinal link

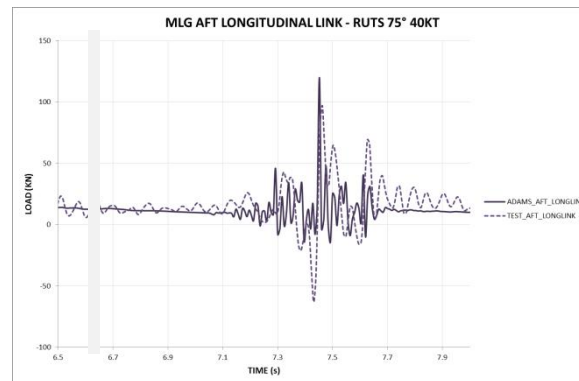


Figure 50: Drag load on AFT longitudinal link. Ruts 15° 40Kt

3.2.3 Conclusions of Ruts model matching

Due to the huge quantity of time-histories analysed during this matching process, with two different rut angles and three taxiing speeds is enough to extract a solid conclusion.

The dynamic response by double excitation due to pass over this double obstacle is reproduced with enough accuracy in the mostly of checked monitoring stations. The model shows good correlation for the attachment and ground loads either on the NLG and MLG.

The adjusting is fulfilled in a general view since peak levels and frequency achieve a good correlation with flight test results. The process is passed qualitative and quantitative evaluation of the correlation overview.

Besides, the mostly of checking process in monitoring stations shows conservative values for computing model with respect to flight test results.

4. A/C CAPABILITY

This chapter studies the A/C capability based on validated model in §3.

In this process extended A/C weight up to MTW are carried out with application of limitations in the obstacle severity in case load exudences

Study coverage in terms of tyre bottoming for maximum weight operation of tyre pressure servicing class A & B are taking into account (Low pressure condition on tyres)

4.1 Considerations in the models with non-low CBR

The current matching model has been validated for low CBR. The capability extends the study to every type runway independently of material is made. Therefore in order to be conservative and to cover every type runway pavement mechanical characteristics are assumed in term of loads. In other words the obstacle profile is undeformable.

Next implications have been taken into account:

- Reaction corner has been assumed with respect to low CBR matching model with any factor reduction.
- Ground damping has been removed as pavement mechanical characteristics are assumed.
- Profile distortion disappears.
- Tyre pressure servicing class is set to C. (standard tyre pressure)

- Tyre expansion along the ruts and pothole are revised for assumed rigid pavement to take into account the effect of undeformable geometry. According to the last point, the "Lgeo" parameter had to be fitted to meet the tire expansion expected.
- Potholes: It has been assumed slope of 20 deg in the pothole profile before and after the pothole corners.

4.2 Pothole capability

The general capability of the A/C is obtained for extended weights up to MTW

The first step consists to sweep the length diameter for the whole speed range up to 60kt to evaluate the critical cases at each velocity. Above 60kt lift is reducing loads.

The pothole computing envelope is covering diameters up to 3m. Above that it is assumed as step
The tyre pressure selected for the capability study is Servicing Class C (tyre Standard pressure)

4.2.1 Low CBR runways at 115t

Checking between LGs design limit loads and the pothole loads envelope parametrized in function of A/C speed with A/C weight at 115 tons

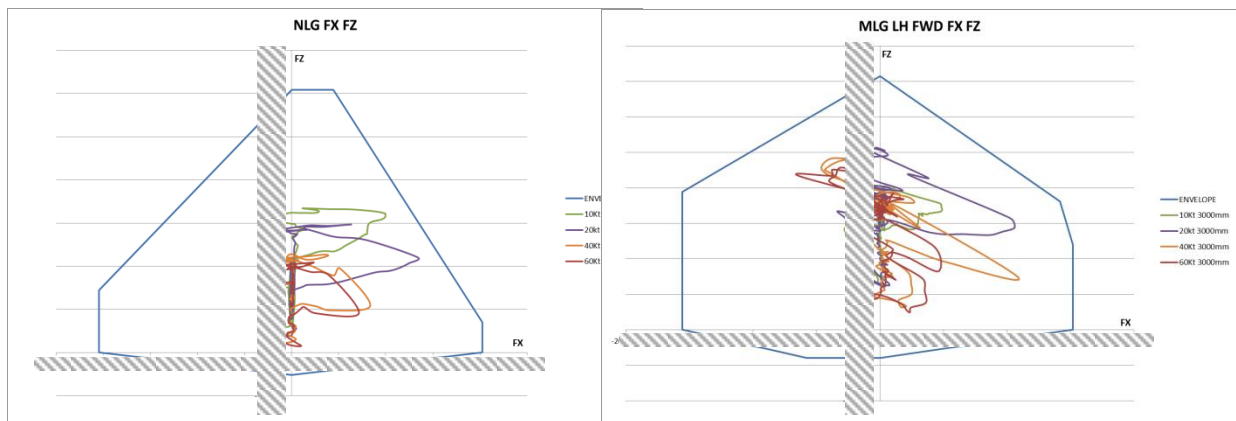


Figure 51: FXZ Envelope NLG & FWD legs. Pothole Low CBR

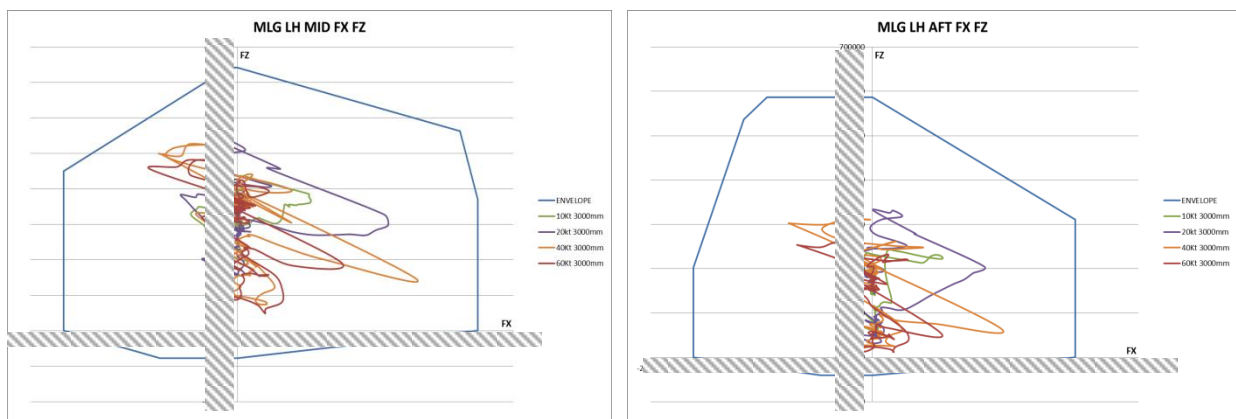


Figure 52: FXZ Envelope MID & AFT. Pothole Low CBR

Conclusions: All critical load cases are inside the envelopes. The operation over potholes at low CBR up to A/C weight of 115 tons is demonstrated.

4.2.2 Non Low CBR runways at 115 tons

Checking loads is verified versus design limit loads envelopes for the NLG and MLG structure
The assumptions reported in §4.1 has been implemented for non-low CBR capability.
All the simulations computed with non-low CBR for the runways are assumed as a rigid pavement.

Conclusions: All critical load cases are inside the envelopes. The operation over potholes at non-low CBR runways up to A/C weight of 115 tons is demonstrated and therefore, it is covering in loads non-low CBR runways.

Note: In case of non-low CBR runways, tyre Servicing Class C is recommended to avoid bottoming conditions in pothole / rut operations.

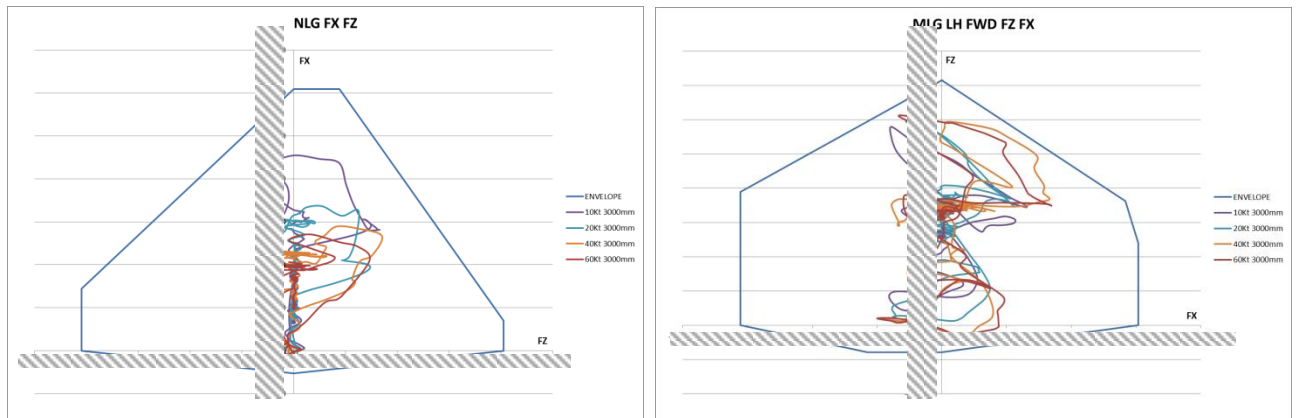


Figure 53: FXZ Envelope NLG & FWD legs. Pothole Non-Low CBR

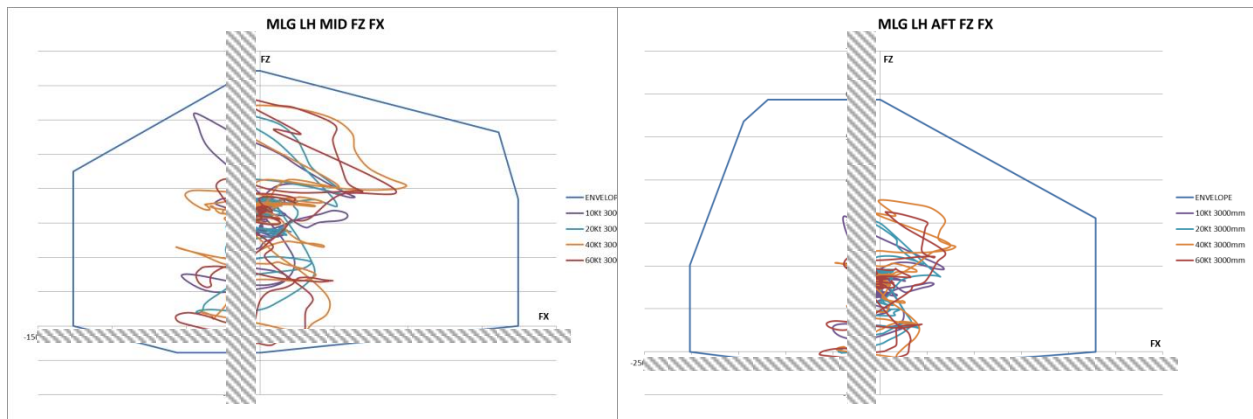


Figure 54: FXZ Envelope MID & AFT legs. Pothole Non-Low CBR

4.2.3 Extended weight capability beyond 115t

The extended A/C weight capability up to MTW has been included with the necessary limitations in pothole depth from loads point of view.

An iterative process by the reduction of pothole depth in weight function is carried out for extended weights beyond 115 tons

4.3 Capability for Operation on runways crossing over Ruts

The general capability of the A/C is obtained for extended A/C weights up to MTW

A sweeping process of the orientation of rut line angle between 15 to 90 deg is taken for the whole speed range up to 60kt; above 60kt lift is reducing loads.

The tyre pressure selected for the capability study is Servicing Class C. (Tyre standard pressure)

4.3.1 Rut profiles

The different rut profiles that can be found in real life on the unpaved runways in term to study the A/C capability have been classified into three types depending of lateral wandering and lateral wall slope.

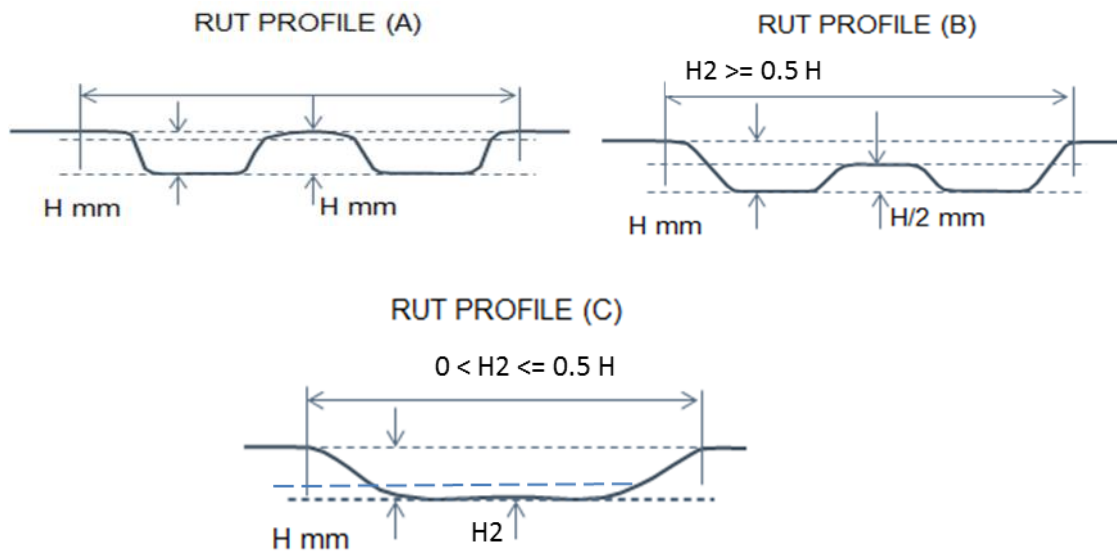


Figure 55: Classification of Rut Profiles

The Profile (A) is typical for low CBR runways, but depending of the dry/wet conditions of the terrain the existence of each profile type shall be taken into account.

4.3.2 Low CBR runways up to 115 tons

The parameters used to validate the model for ruts angle at 15 deg and 45 deg, are also used to calculate the capability of the aircraft for the whole sector (from 0 to 90 deg).

In the next graphic envelopes is identified A/C of speed critical for every rut angle.

The following figures show the envelopes FXY, FXZ and FYZ for critical cases either for the NLG and MLG.

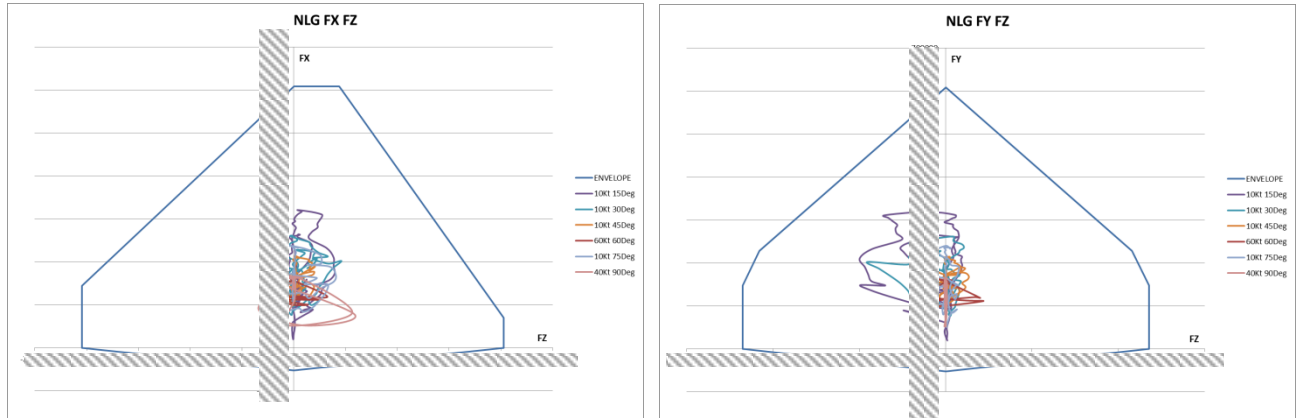


Figure 56: NLG leg FXZ & FYZ envelope. Rut Low CBR

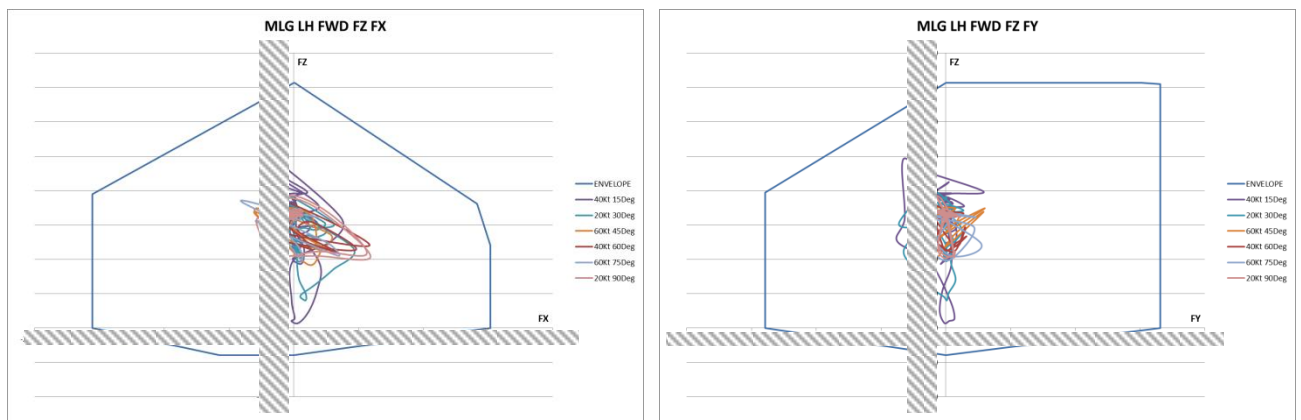


Figure 57: FWD leg FXZ & FYZ envelope. Rut Low CBR

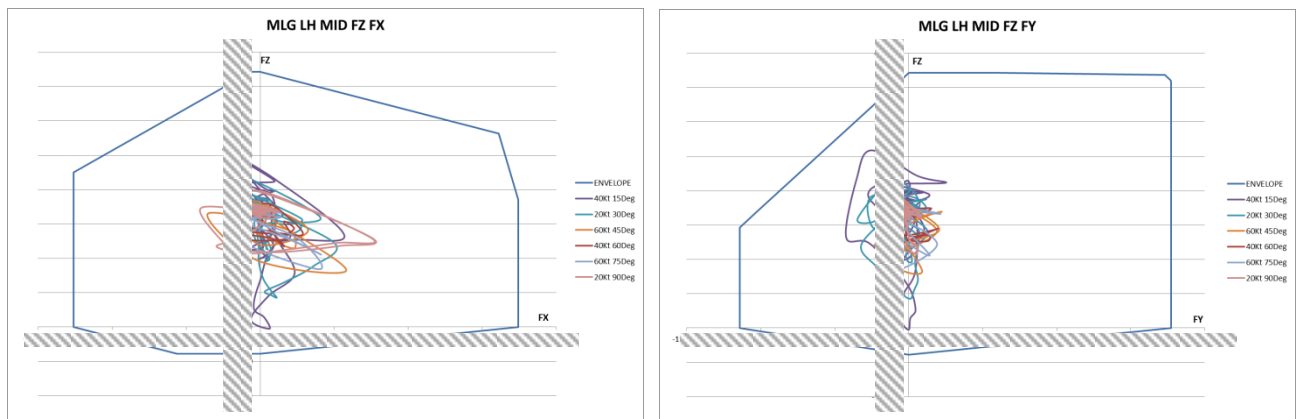


Figure 58: MID leg FXZ & FYZ envelope. Rut Low CBR

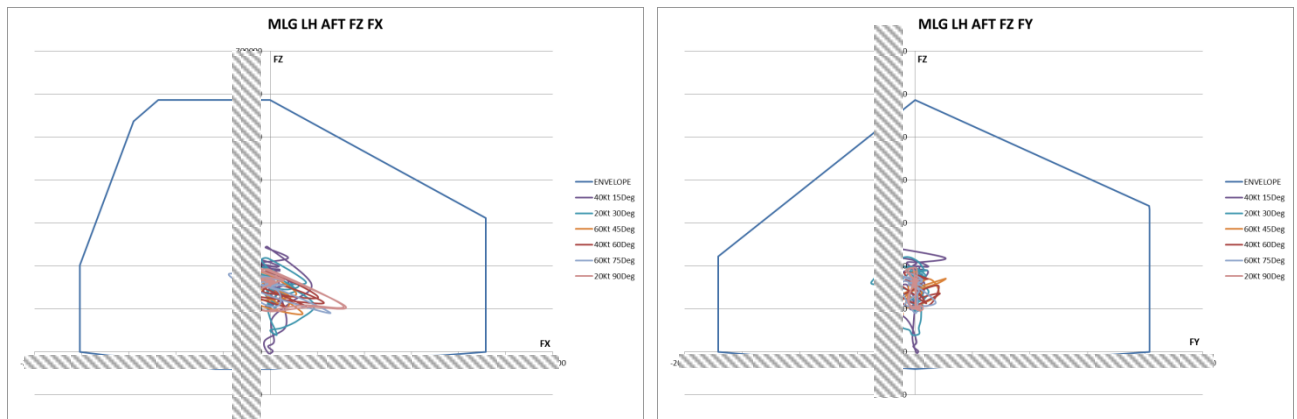


Figure 59: AFT leg FXZ & FYZ envelope. Rut Low CBR

Conclusions: All critical load cases are inside the limit loads envelopes. The operation of crossing over ruts at low CBR up to A/C weight of 115 tons is covered at any angle.

4.3.2.1 Rut Profile limitation

All computations have been performed with type profile A.

- Type profile (A) is covering rut depth up to 200 mm
- Limitation of rut depth to 100 mm is applied for rut type profile (B) & (C) based in potholes capability.

4.3.3 Non Low CBR runways up to 115 tons

Checking loads comparison between design limit loads and the ruts loads envelope in case of non-low CBR runways,

The assumptions reported in §4.1 has been implemented for non-low CBR capability.

It is important to remember that for all the simulations run in runways with non-low CBR the terrain is assumed as a rigid pavement in order to be conservative in loads.

4.3.3.1 Application of limitation in function of rut line angle

According to geometry considerations reported into § 2.5.4 in terms of rut angle orientation over the runway, knowing that tyre expansion is hardly dependent of rut angle facing to, the rut depth limitation shall be applied.

In the case of ruts under non-low CBR conditions the angle rut cases are differentiated in two sectors:

- Sector (A) from 90 deg (perpendicular to A/C long. axis) to 60 deg; the wheel does not drop into the rut and then the rut height is set to 200mm.
- Sector (B & C) from 60 deg to almost parallel to the A/C longitudinal axis; the wheel is assumed to drop partially or totally into the rut then the rut height is limited to 100mm.

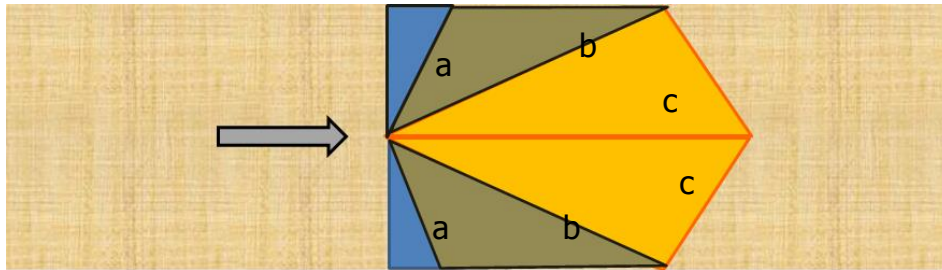


Figure 60: Classification of angle rut sectors along Runway

4.3.3.2 Envelopes of sector (A) . Crossing ruts from 90 to 60 deg

Simulations with ruts model case (a). Identical A/C speed critical cases in function of rut angle for low CBR are run in non-low CBR conditions.

Below are shown the envelopes FXY, FXZ and FYZ for critical cases either for the NLG and MLG.

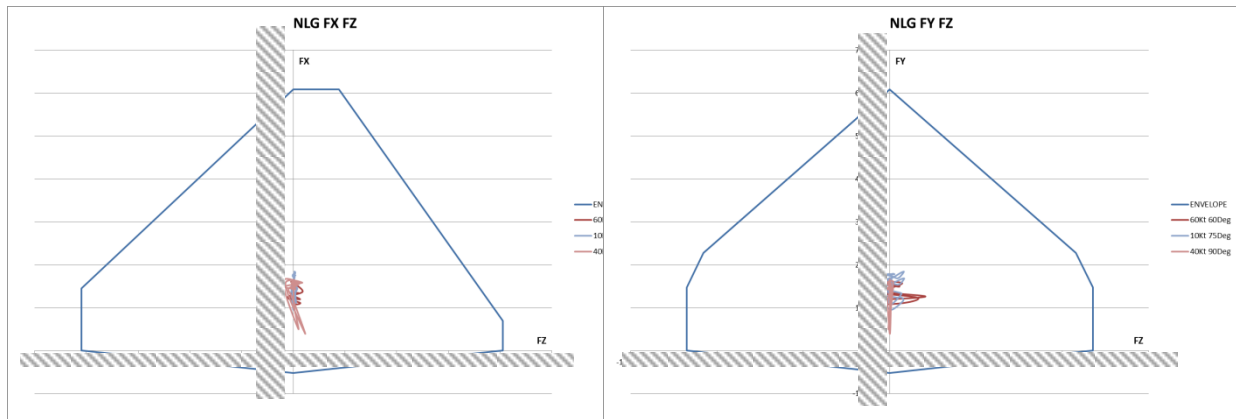


Figure 61: NLG FXZ & FYZ Envelope. Rut Non-Low CBR

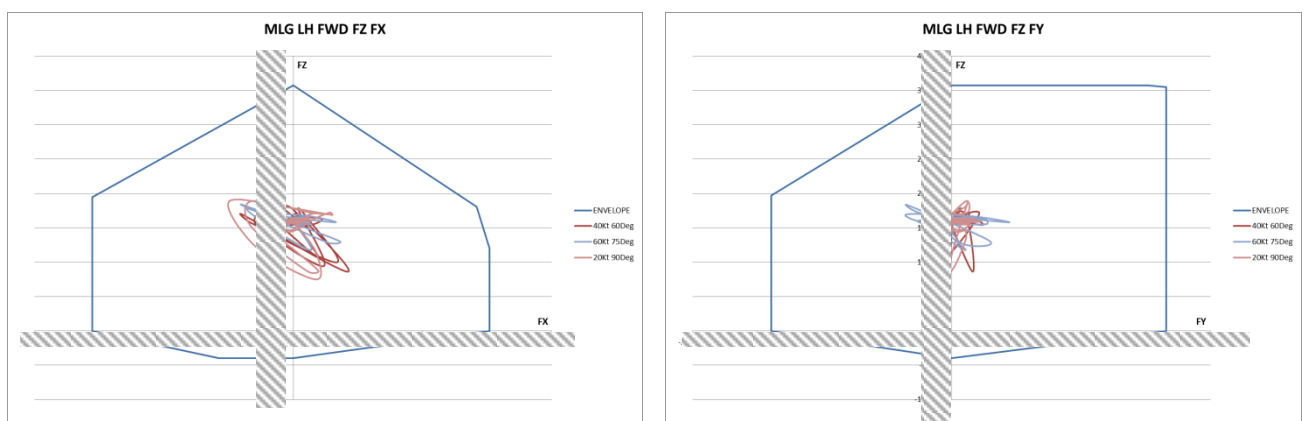


Figure 62: FWD FXZ & FYZ Envelope. Rut Non-Low CBR

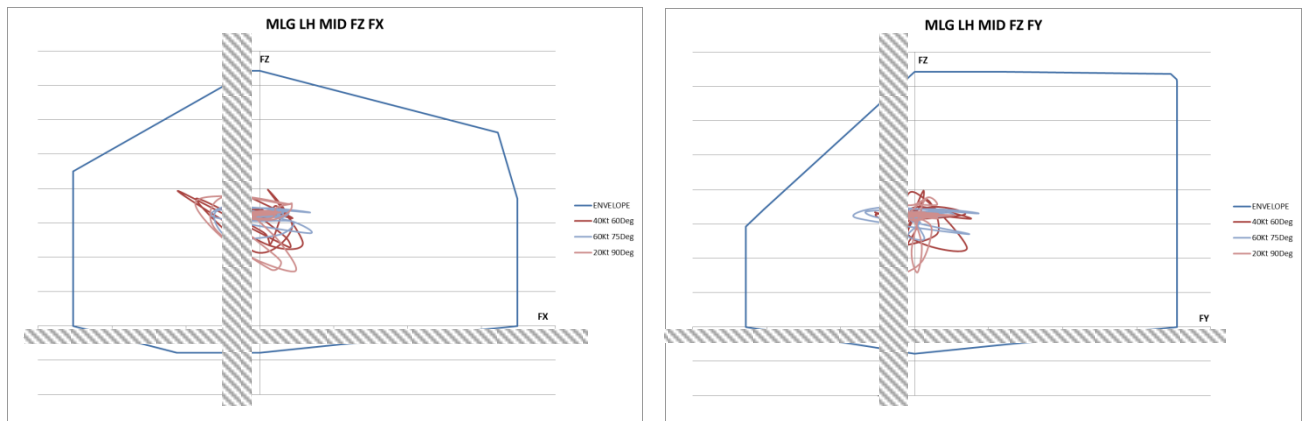


Figure 63: MID FXZ & FYZ Envelope. Rut Non-Low CBR

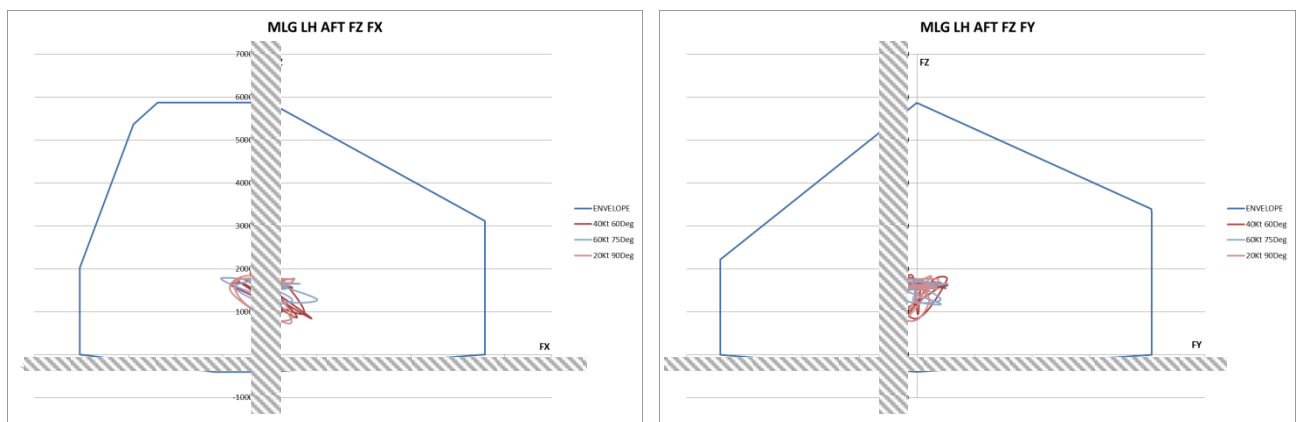


Figure 64: AFT FXZ & FYZ Envelope. Rut Non-Low CBR

4.3.3.3 Envelopes of sector (B & C) . Crossing ruts from 60 to almost parallel to runway.

Rut depth is limited up to 100 mm.

These computations are covered in loads by the pothole envelope for High CBR conditions with the simulations made with 100 mm in height and a range up to 3000 mm in length.

The loads on ruts rut is covered by the pothole as equal height conditions as the wheel drops partially into the rut in contrast to the pothole case where the wheel always drops totally.

4.3.3.4 Rut Profile limitation

All computations have been performed with type profile A.

- Type profile (A) is covering rut depth up to 200 mm only for sector (a) See Figure 60
- Type profile (A) is covering rut depth up to 100 mm only for any angle into the sector sectors (b) and sector (c) -See Figure 60
- Limitation of rut depth to 100 mm is applied for rut type profile (B) & (C) for any rut angle (all sectors) based in potholes capability for non-low CBR runways

4.3.4 EXTENDED A/C WEIGHT CAPABILITY BEYOND 115T FOR RUTS OPERATION

Extended A/C weight capability up to MTW tons is computing with the necessary limitations in pothole depth from loads point of view.



5. OPERATIONAL CAPABILITY FOR ANY TYPE OF RUNWAYS

The capability of the operation over different terrain discontinuities (potholes, ruts, or short bumps) are going to be uniformed independently of type of runway and will enclose every rut profile shape and orientation that A/C can find along its ground operations.

Additionally, and in order to cover all certified tyre pressures, the limitation is extended to Servicing Class D, whose using will be more limiting than SC. C. (high tyre pressures)

For Servicing Class A and B (Ref.6) capability operation is included on next chapters always taking into account the A/C weight limitation per each tyre pressure SC A or SC B. (Low tyre pressure selection)

5.1 Pothole operational capability

The capability tables are separated for high pressures and low pressures to give clearer the envelopes. This table is built based on results extracted from §4.2 aver valid to SC C and SC D

DISTRESS TYPE	CLASSIFICATION	DESCRIPTION: operation on runways crossing over Potholes. Servicing Class C and D
POTHOLES	GREEN (*)	<p>VALID FOR ALL TYPE OF RUNWAYS <u>Limitations applicable for tyre pressure SC C and SC D</u> (high tyre pressures)</p> <ul style="list-style-type: none"> ❖ Any pothole with diameter less than 300mm ❖ Pothole with diameter greater than 300mm: <ul style="list-style-type: none"> Pothole depth limitation to 100mm with A/C weight up to W1 Pothole depth limitation to 76mm with A/C weight at W2 <ul style="list-style-type: none"> • Between W1 and W2 linear interpolation is applied to define the limit pothole deep capability. Pothole limitation to 50mm with A/C weight at W3 <ul style="list-style-type: none"> • Between W2 and W3 linear interpolation is applied to define the limit pothole deep capability.
	RED	<p>Pothole with diameter greater than 300mm and any operational point that exceeds area envelope in the above figure.</p>

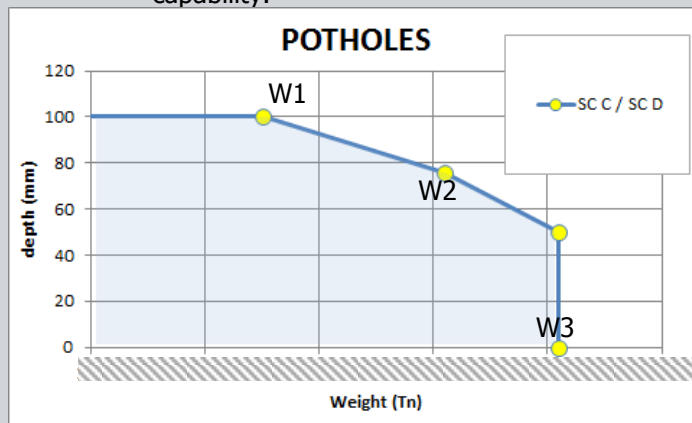


Table 4: Operational Capability over pothole using high tyre pressure

(*) Green defines the conditions to give clearance to the operation.

This table is built based on results extracted from §4.2 and are valid to SC A and SC B
Taking into account weight limitations for low tyre pressure of Ref.11

DISTRESS TYPE	CLASSIFICATION	DESCRIPTION: operation on runways crossing over Potholes LOW TYRE PRESSURE Servicing Class A and B
POTHOLES	GREEN (*)	<p><u>Limitations applicable for tyre pressure SC A</u></p> <ul style="list-style-type: none"> ❖ Any pothole with diameter less than 300mm ❖ Pothole with diameter greater than 300mm : If CBR0 < 10 (1st layer terrain between 0 to 10 cm) Pothole depth limitation to 100mm with A/C weight up to W1 For any CBR Pothole depth limitation to 50mm with A/C weight up to W1 <p><u>Limitations applicable for tyre pressure SC B</u></p> <ul style="list-style-type: none"> ❖ Any pothole with diameter less than 300mm ❖ Pothole with diameter greater than 300mm : If CBR0 < 10 (1st layer terrain between 0 to 10 cm) Pothole depth limitation to 100mm with A/C weight up to W1 <ul style="list-style-type: none"> • Between W1 and W2 linear interpolation is applied to define the limit pothole deep capability. <p>For any CBR Pothole depth limitation to 50mm with A/C weight up to W2</p> <div data-bbox="676 1111 1396 1541" style="text-align: center;"> </div>
	RED	Pothole with diameter greater than 300mm and any operational point that exceeds area envelopes in the above figure.

Table 5: Operational Capability over pothole using low pressure on tyres

Note: if a pothole whose depth is higher than 50 mm is found in a hard point (CBR0 > 10) on a soft runway, this pothole must be repaired if low pressure want to be used (SC A or SC B)
CBR0 is the CBR measurements according to 1st terrain layer between 0 mm and 100 mm

(*) Green defines the conditions to give clearance to the operation.

5.2 Operational capability for operation on runways over crossing Ruts

This table is built based on results extracted from §4.3

DISTRESS TYPE	CLASSIFICATION	DESCRIPTION: operation on runways over crossing Ruts
CROSSING OVER RUTS	GREEN (*)	<p>VALID FOR ALL TYPE OF RUNWAYS VALID FOR ALL SHAPE OF RUT PROFILE VALID FOR ANY RUT CROSSING ANGLE</p> <ul style="list-style-type: none"> ➤ <u>Limitations applicable for tyre pressure SC C & SC D</u> Ruts depth limitation to 100mm with A/C weight up to W1 Ruts depth limitation to 38mm with A/C weight at W3 <ul style="list-style-type: none"> • Between W1 and W3 linear interpolation is applied to define the limit rut depth capability. ➤ <u>Limitations applicable for tyre pressure SC A</u> Ruts depth limitation to 100mm with A/C weight up to W1 ➤ <u>Limitations applicable for tyre pressure SC B</u> Ruts depth limitation to 100mm with A/C weight up to W1 Ruts depth limitation to 60mm with A/C weight at W2 <ul style="list-style-type: none"> • Between W1 and W2 linear interpolation is applied to define the limit rut depth capability.
	RED	Any operational point that exceeds area envelopes in the above figure

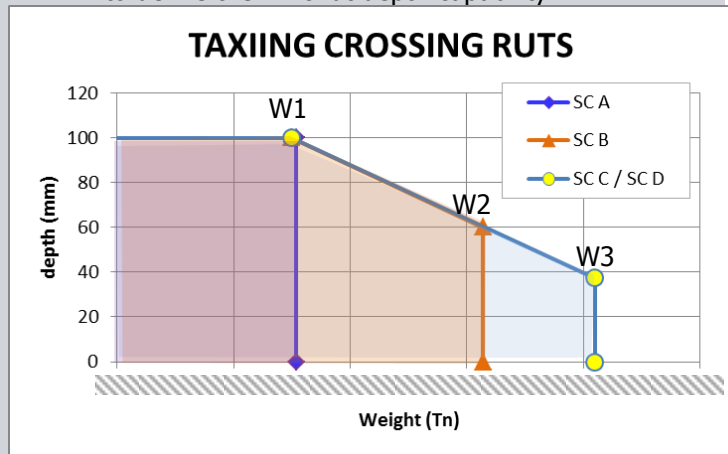


Table 6: Operational Capability for A400M taxiing over crossing ruts

(*) Green defines the conditions to give clearance to the operation

6. CONCLUSIONS

The complexity of the model due to large quantity of parameters that are leading the physical behaviour makes more relevant this achieved objective.

The accuracy degree in the correlations has been enough to complete the A/C capability into the certification plan for the unpaved operation runways of A400M

The great success to achieve a good correlation between this mathematical model for ground obstacles has not only been to accomplish the A/C capability for these ground discontinuities, but besides a way to extend this capability for future studies is opened without the necessity to perform a complete and dedicated flight tests campaign with associated saving costs.

REFERENCES:

- 1.– Airbus Presentation, "Taxi Runs On Standard Bump Franczal 30/31-08-2010".
- 2.– Silvia Parra Adan; July 2017; TAE-A4-NT-160613, Flight Test Request - A400M: Turnings and Potholes for Unpaved Runways Step3 Campaign
- 3.– Isabelle Desfond; 2017; "A400M WOODBRIDGE CHARACTERIZATION" MMMURWA0017C12 issue1.0 v3.0
- 4.– Gary C. Gibson & Harry M. Coyle; September 1968;. RESEARCH REPORT 125-1 STUDY 2-5-67-125, SOIL DAMPING CONSTANTS RELATED TO COMMON SOIL PROPERTIES IN SANDS AND CLAYS" The Texas Highway Department In Cooperation with the U. S. Department of Transportation, Federal Highway Administration, Bureau of Public Roads.
- 5.– Esteban Gomez; April 2013; ME-A4-NT-120619_Issue B, "MODEL OF REACTION FORCE FOR TAXIING OVER BUMP PROFILE OF SINGLE STEP"
- 6.- M00RP1517997; June 2015; "A400M Tire/Runway Lateral Friction coefficients"
- 7.-Silvia Parra Adan; 2014; ME-A4-NT-130249 Issue B, "A400M STEP BUMP CAPABILITY"